electronics

MDPI

Article

Economic and Ecological Design of Hybrid Renewable Energy Systems Based on a Developed IWO/BSA Algorithm

Mohammed Kharrich [1], Salah Kamel [2], Rachid Ellaia [3], Mohammed Akherraz [1], Ali S. Alghamdi [4,*], Mamdouh Abdel-Akher [2,5], Ahmad Eid [2,5] and Mohamed I. Mosaad [6]

1 Department of Electrical Engineering, Mohammadia School of Engineers, Mohammed V University in Rabat, Ibn Sina Street P.B 765, Rabat 10090, Morocco; mohammedkharrich@research.emi.ac.ma (M.K.); akherraz@emi.ac.ma (M.A.)
2 Department of Electrical Engineering, Faculty of Engineering, Aswan University, Aswan 81542, Egypt; skamel@aswu.edu.eg (S.K.); mabdelakher@ieee.org (M.A.-A.); ahmadeid@aswu.edu.eg (A.E.)
3 LERMA Laboratory, Engineering for Smart and Sustainable Systems Research Center, Mohammadia School of Engineers, Mohammed V University in Rabat, Ibn Sina Street P.B 765, Rabat 10090, Morocco; rachid.ellaia@gmail.com
4 Department of Electrical Engineering, College of Engineering, Majmaah University, Al-Majmaah 11952, Saudi Arabia
5 Department of Electrical Engineering, Unaizah College of Engineering, Qassim University, Unaizah 56453, Saudi Arabia
6 Department of Electrical and Electronic Engineering, Yanbu Industrial College, Yanbu 46452, Saudi Arabia; habibm@rcyci.edu.sa
* Correspondence: aalghamdi@mu.edu.sa

Citation: Kharrich, M.; Kamel, S.; Ellaia, R.; Akherraz, M.; Alghamdi, A.S.; Abdel-Akher, M.; Eid, A.; Mosaad, M.I. Economic and Ecological Design of Hybrid Renewable Energy Systems Based on a Developed IWO/BSA Algorithm. *Electronics* **2021**, *10*, 687. https://doi.org/10.3390/electronics10060687

Academic Editors: Md Alamgir Hossain, Ripon Kumar Chakrabortty and Stefano Squartini

Received: 8 February 2021
Accepted: 8 March 2021
Published: 15 March 2021

Abstract: In this paper, an optimal design of a microgrid including four houses in Dakhla city (Morocco) is proposed. To make this study comprehensive and applicable to any hybrid system, each house has a different configuration of renewable energies. The configurations of these four houses are *PV*/wind turbine (*WT*)/biomass/battery, *PV*/biomass, *PV*/diesel/battery, and *WT*/diesel/battery systems. The comparison factor among these configurations is the cost of energy (COE), comparative index, where the load is different in the four houses. Otherwise, the main objective function is the minimization of the net present cost (*NPC*), subject to several operating constraints, the power loss, the power generated by the renewable sources (renewable fraction), and the availability. This objective function is achieved using a developed optimization algorithm. The main contribution of this paper is to propose and apply a new optimization technique for the optimal design of a microgrid considering different economic and ecological aspects. The developed optimization algorithm is based on the hybridization of two metaheuristic algorithms, the invasive weed optimization (IWO) and backtracking search algorithm (BSA), with the aim of collecting the advantages of both. The proposed hybrid optimization algorithm (IWO/BSA) is compared with the original two optimization methods (IWO and BSA) as well as other well-known optimization methods. The results indicate that *PV*/biomass and *PV*/diesel/battery systems have the best energy cost using the proposed IWO/BSA algorithm with 0.1184 $/kWh and 0.1354 $/kWh, respectively. The best system based on its *LCOE* factor is the *PV*/biomass which represents an *NPC* of 124,689 $, the size of this system is 349.55 m^2 of *PV* area and the capacity of the biomass is 18.99 ton/year. The *PV*/diesel/battery option has also good results, with a system *NPC* of 142,233 $, the size of this system is about 391.39 m^2 of *PV* area, rated power of diesel generator about 0.55 kW, and a battery capacity of 12.97 kWh. Otherwise, the proposed IWO/BSA has the best convergence in all cases. It is observed that the wind turbine generates more dumped power, and the *PV* system is highly suitable for the studied area.

Keywords: hybrid renewable energy system; *PV*; wind energy; battery energy storage; biomass system; invasive weed optimization algorithm; backtracking search algorithm

1. Introduction

Increasing power demand is a logical result of the significant increase in the world population and their energy consumption and industrialization growth. Distributed systems-based-renewable energy resources appear as a practical solution compared with the traditional energy resources due to the advantages of using such renewable sources. A microgrid is a distribution system consisting of hybrid energy sources dedicated to meet a particular need for electrical energy. A microgrid can be isolated from the utility in most cases; otherwise, it can be connected to the network when the microgrid owner needs more power flexibility. The authors of [1] presented the major issues regarding the motivations and benefits of adopting hybrid renewable energy systems (HRES), mainly in sub-Sahara Africa. Different renewable energy systems that can be adopted for HRES applications for both on-grid and off-grid consumers were proposed and discussed. Detailed design and modeling of an isolated HRES have been presented in [2], including traditional and renewable energy resources using meta-heuristic algorithms. Additionally, the technical and ecological factors have been considered. Other pertinent review research, such as microgrid transactive energy [3], optimal smart energy coordination in the microgrid applications [4], multi-agent microgrid management system for single-board computers [5], and peer-to-peer energy trading in micro/mini-grids for local energy communities [6], statistical analysis of PV/wind HRES have been presented in [7].

Investing in renewable energy systems is not an easy issue as it has several aspects, including the economic aspect, which have emerged as a result of the global economic crises and the technical aspects related to the stability and continuity of energy supply from renewable sources, especially the sources which depend on variable environmental conditions (wind, sunlight).

The first and vital obstacle that must be avoided is to find the best design of the system. The optimal design of microgrid means that the project owner should evaluate the whole region and all sources available. Consequently, the design should be economical and follow many technical aspects and environmental criteria.

In the literature, many studies were presented for several locations, each promoting its appropriate system. In [8], the authors implemented different recent algorithms—whale optimization algorithm (WOA), water cycle algorithm (WCA), moth-flame optimizer (MFO), and hybrid particle swarm-gravitational search algorithm (PSOGSA)—to design a PV/wind/diesel/battery microgrid system through minimizing the cost of energy and increasing the reliability and efficiency of the system. In [9], the authors focused on wind/biomass/diesel/battery stand-alone microgrids and discussed the system operation, energy management, and dispatch issues in detail. In [10], the authors designed a microgrid system with the same load in two different countries to assess the effect of the metrological conditions and compare the cost of energy for both systems. An optimization algorithm to reduce the operational cost of a hybrid residential microgrid consisting of a diesel generator, WT and PV array, and battery energy storage system has been presented in [11]. In [12], the authors applied a grasshopper optimization algorithm to design an autonomous microgrid system containing PV/WT/battery/diesel generator. The reliability is studied using the deficiency of power supply probability (DPSP) factor, while the GOA has been compared with PSO and cuckoo search. The firefly algorithm has been used to find the optimal hybrid system configuration to feed three un-electrified remote villages [13]. The optimization method presented for minimizing the cost of energy considering the loss of load probability (LOLP) reliability index for a hybrid PV/WT/battery system. In [14], the optimal sizing of the hybrid renewable energy system (HRESs) in a remote area composed of PV/WT/battery/diesel has been developed using the social spider optimizer algorithm. The social spider optimizer (SSO) algorithm has been compared with many algorithms including Harris Hawks optimizer (HHO), grey wolf optimizer (GWO), multi-verse optimizer, antlion optimizer (ALO), and whale optimization algorithm. The IWO and BSA have been used to solve many problems, such as the unit commitment (UC) [15] and the economic environmental power dispatch problems [16]. Likewise, the IWO and BSA have been hybridized many times with other algorithms to get better performance. The IWO has been hybridized with IPSO for mobile robot's navigation in a dynamic environment [17]. Also, it has been hybridized with the WDO algorithm for nulling pattern synthesis of uniformly spaced linear and non-uniform circular array antenna [18]. Otherwise, the BSA has been hybridized for permutation flow-shop scheduling problem [19].

Despite the development and continuous improvement in the optimization techniques, there are still continuous attempts to achieve better results by updating the existing optimization algorithms, proposing new optimization algorithms, inspired by biological or social behaviors, or hybridizing more than one algorithm advantages of all of them. In [20], a hybrid algorithm of Jaya and teaching–learning-based optimization (JLBO) named the JLBO algorithm has been proposed for the optimal unit sizing of the hybrid PV/WT/battery system to feed electricity to a remote area. In [21], a modified bonobo optimizer (BO) algorithm has been proposed to have more ability in exploitation and exploration phases. The developed version is called the quasi-oppositional BO (QOBO). The developed algorithm has been introduced to design several scenarios for the HRESs. In [22], a modified crow search algorithm (CSA) has been proposed for optimizing a hybrid PV/diesel/PHS system, considering the fuel consumption as an objective function. The proposed approach has been compared with the particle swarm optimization, genetic algorithm, and the original CSA. A multi-objective-based optimization algorithm called BOACA has been proposed in [23], to reduce cost, emissions and find the best configuration of HRESs. The results obtained by BOACA have been compared with GA, PSO, and HOMER. In [24,25], the multi-objective evolutionary algorithm has been applied for the optimal design and the optimal allocation of the HRES, respectively. In [26], the optimal design and operating schedule has been presented to meet the energy demand of Pantelleria island. In [27], a modified particle swarm optimisation algorithm has been proposed for energy management of microgrid under uncertain environments. In [28], a mathematical approach has been developed to assess the potential of electricity production, exploiting from the available sources such as solar, wind speed, and sea wave in the Balearic and Fiji islands. In [29], HOMER has been used to investigate the techno-economic feasibility analysis of several HRES in Pratas Island (Taiwan). In [30], HOMER has been used to design an optimal HRES in Muhavoor, India. Several configurations have been considered based on PV, WT, diesel and battery. In [31], HOMER has been used to design a HRES of PV, WT, diesel and battery to avoid the diesel emission problems in Malaysia. In [32], a novel energy-economic-environmental multi-criteria decision framework has been developed for a HRES optimization. In [33], a mathematical model has been proposed to get the optimal energy mix in Lampedusa, Italy. In [34], a cost-efficient optimization algorithm has been proposed to maximize the RE penetration and find the optimal sizing of the HRES.

Table 1 summarizes the usage of hybrid optimization techniques in RESs. This paper aims at optimal economic and ecological design of a microgrid using a proposed hybrid optimization technique, IWO/BSA. The proposed microgrid consists of four houses in the city of Morocco. This microgrid includes different combinations of energy resources, namely PV, wind, biomass, diesel, and battery energy storage. Besides the optimal design presented in this paper, the penetration level of HRESs, the power supply availably and continuity are considered. To assess the effectiveness and performance of the proposed optimization technique, a comparison with different optimization algorithms is presented. However, the main contribution of this paper can be summarized in the following points:

- We propose a hybrid algorithm called IWO/BSA, with the aim of improving the performance of the original IWO and BSA algorithms by combining their advantages into an algorithm.
- The proposed algorithm is applied to the optimal economic design of a stand-alone hybrid microgrid system in Dakhla (Morocco).
- Four configurations consisting of RES (PV, WT and biomass) with diesel generators and battery storage systems are suggested.

Table 1. Summary of reported methods in optimizing HRESs.

Reference	Year	Hybrid RESs	Algorithm/Tool	OF	Advantages	Potential Improvements
Tooryan et al. [11]	2020	*PV*/wind/diesel/battery	PSO, GA	*NPC*	Clear and simple study	Classical approach methods are used.
Bukar et al. [12]	2019	*PV*/wind/diesel/battery	GOA, CSA, PSO	COE	Application of GOA algorithm	System credibility such as uncertainty and availability should be enhanced.
Sanajaoba et al. [13]	2019	*PV*/wind/battery	FA, GA, PSO	COE	The developed model is applied for three remote unelectrified villages	The sensitivity analysis is not included.
Fathy et al. [14]	2020	*PV*/wind/battery/diesel	GWO, MVO, ALO, WOA, SSO	COE	Detailed study with many results	The proposed SSO could be further explored
Khan and Javaid [20]	2020	-*PV*/wind/battery -*PV*/battery -Wind/battery	Jaya, TLBO, JLBO, GA	TAC	Proposed a new hybrid algorithm named JLBO	The uncertainty for the wind and *PV* should be considered.
Kharrich et al. [21]	2020	-*PV*/wind/diesel/battery -*PV*/biomass -*PV*/diesel/battery -wind/diesel/battery	QOBO, BO, HHO, AEFA, IWO	*NPC*	Proposed a new developed algorithm called QOBO	The uncertainty parameter is missing.
Makhdoomi and Askarzadeh [22]	2020	*PV*/diesel/PHS	GA, PSO, CSA, CSAAC-AP	Fuel consumption	Proposing a modified CSA	The operation time-span of the study is only 24 h.
Abo-Elyousr and Nozh [23]	2018	*PV*/wind/biomass/NGFC/NGT	BOACA, GA, PSO, HOMER	-COE -GHG	Developing a BOACA algorithm offers optimal HMG system configuration and sizing	The *LPSP* results should be further examined and analyzed.
Hossain et al. [31]	2016	*PV*/wind/diesel/battery	HOMER	*NPC*	Performance evaluation of standalone hybrid system	The study is only based on commercial software application. Other meta-heuristic algorithms could be included and examined.
Heydari and Askarzadeh [35]	2016	*PV*/biomass	HSA	*NPC*	Proving the disadvantage of the HOMER software compared to the meta-heuristic algorithms.	Algorithm comparison is required to confirm that the best results could be found from HS algorithm.
Guangqian et al. [36]	2018	-Wind/*PV*/diesel/battery -Wind/diesel/battery -*PV*/diesel/battery	HSA, SAA, HHSSAA	LCC	Proposing a hybrid algorithm for determining the optimal size of grid-independent system.	The reliability and other factors are should be considered.
Sawle et al. [37]	2018	-*PV*/biomass/diesel/battery -*PV*/diesel/battery -Wind/biomass/diesel/battery -Wind/diesel/battery -*PV*/wind/diesel/battery -*PV*/wind/biomass/diesel/battery	GA, PSO, BFPSO, TLBO	COEI + *LPSP*I + (1/RFI) + (1/HDI) + PMI + (1/JCI)	Considering social, technical, and economic indices in only one objective function.	Adding the uncertainty will bonus and improve this study.

Table 1. *Cont.*

Reference	Year	Hybrid RESs	Algorithm/Tool	OF	Advantages	Potential Improvements
Ramli et al. [38]	2018	*PV*/wind/diesel/battery	MOSaDE	-COE -*LPSP*	Detailed study	Comparison with another multi-objective algorithm is necessary. Otherwise, the knee point should be used to define a compromise solution.
Movahediyan and Askarzadeh [39]	2018	*PV*/diesel	MO-CSA, MOPSO	-*LPSP* -*NPC*-CO2 emission	Considering the operating reserve impact in the sizing problem.	Other systems need to be included in the study.
Ghiasi [40]	2018	*PV*/wind/battery grid connected	MOPSO, MOGA	-Availability -Cost	The use of the availability factor in the inter-connected system.	The reliability could be considered for extending this method.

- Comparing the proposed IWO/BSA with artificial electric field (AEFA), GWO, BSA, and IWO algorithms.

The rest of the paper is organized as follows: Sections 2 and 3 provide the modeling of the systems used in the whole scenarios and the optimization problem formulation, respectively. Section 4 discusses the proposed algorithm. Section 5 describes the case study. Section 6 presents the results and discussions. Finally, the conclusions of the paper are presented in Section 7.

2. Mathematical Description of the Proposed Hybrid System Components

The schematic diagram of the suggested HRES is shown in Figure 1. In this system, four scenarios, including the *PV* power plant, *WT* power plant, diesel generator, biomass, and *BESS* are considered. This microgrid is an AC system as all RESs are linked to the same AC bus. In this study, the DC sources, such as the *PV*, *WT* and *BESS* are linked to the AC bus through DC/AC inverters. The *WT*s also need a controlled inverter to regulate the output power in terms of the specified voltage and frequency.

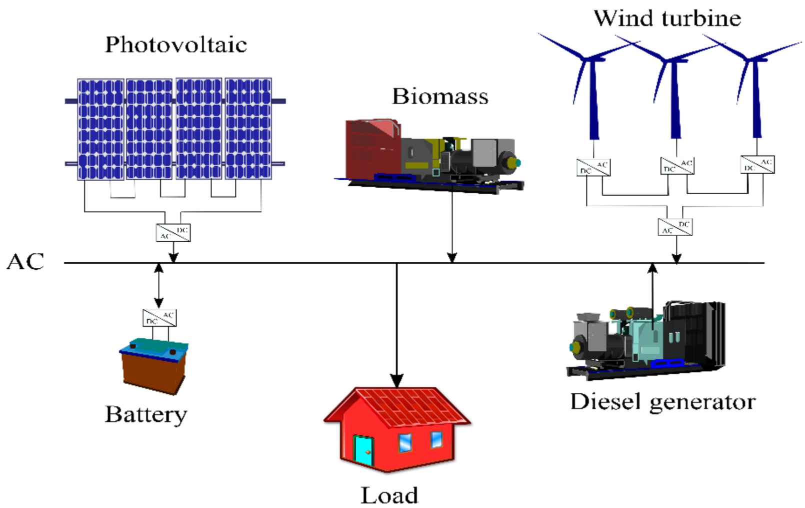

Figure 1. Isolated microgrid system components used for different scenarios.

Two strategies are adopted in this paper; in the first strategy, the combination of biomass/*PV* is considered, as shown in Figure 2. In the second strategy, *PV* or wind or both of them are considered as shown in Figure 3. For either strategy, the proposed operation of the microgrid resources is as:

- The *PV* and *WT* are used firstly as the main power sources to feed the load needs.
- The *BESS* operates when the *PV* and *WT* cannot feed the full load.
- The biomass system starts working when the battery depletes to a minimum permissible power and the load power exceeds 30% of its nominal power.

2.1. PV System

The output power of the *PV* system depends on many parameters as [35]:

$$P_{pv} = I\langle t\rangle \times \eta_{pv}\langle t\rangle \times A_{pv} \tag{1}$$

where, I represents the solar irradiation, A_{pv} represents the *PV* area and η_{pv} is the efficiency of the *PV*, which can be calculated as:

$$\eta_{pv}(t) = \eta_r \times \eta_t \times \left[1 - \beta \times (T_a\langle t\rangle - T_r) - \beta \times I\langle t\rangle \times \left(\frac{NOCT - 20}{800}\right) \times (1 - \eta_r \times \eta_t)\right] \tag{2}$$

where, $NOCT$ is the nominal operating cell temperature (°C), η_r is the reference efficiency, η_t is the efficiency of the MPPT equipment, β is the temperature coefficient of the efficiency,

T_a is the ambient temperature (°C), and T_r is the photovoltaic cell reference temperature (°C).

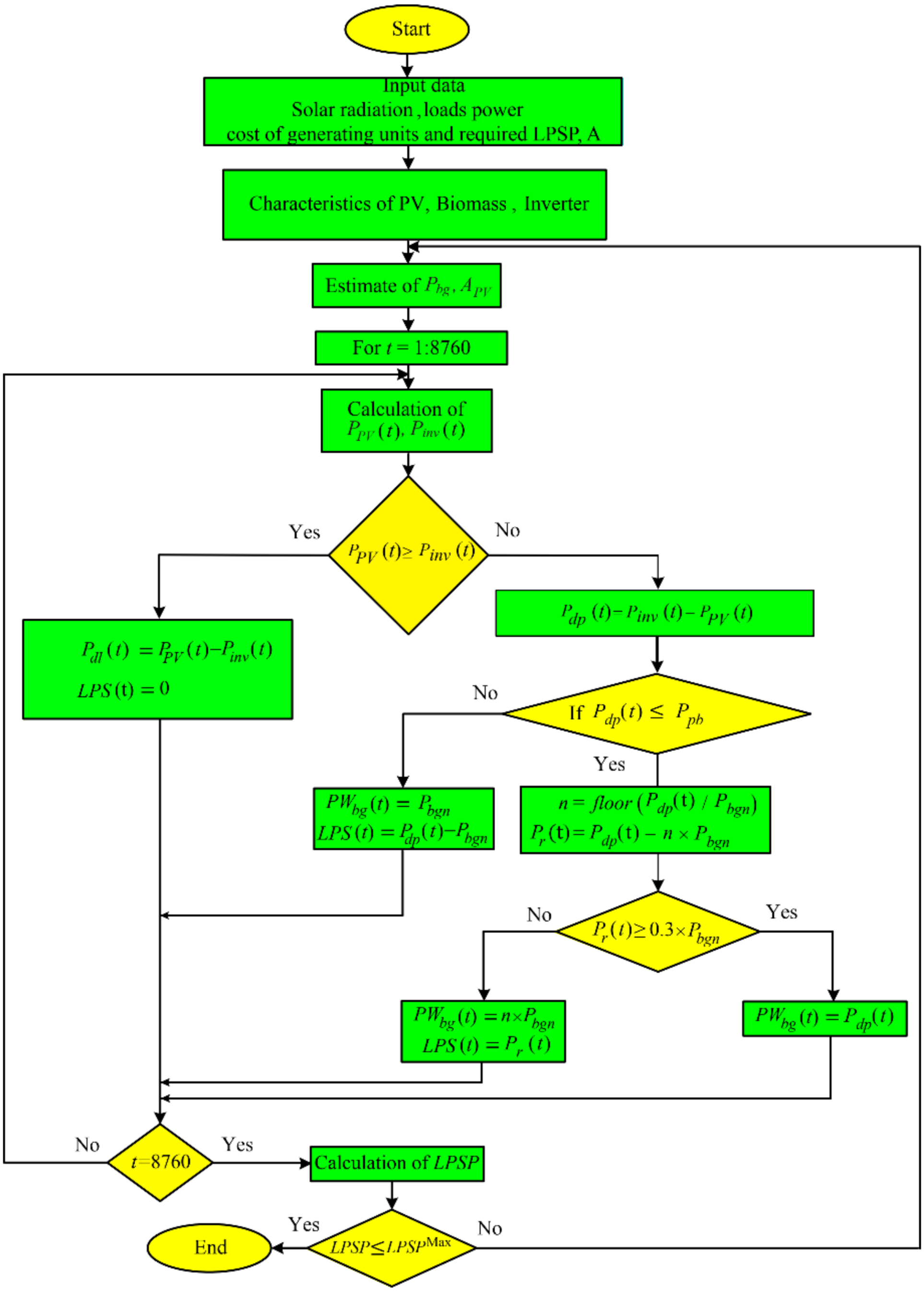

Figure 2. Power management of the PV/Biomass HRES.

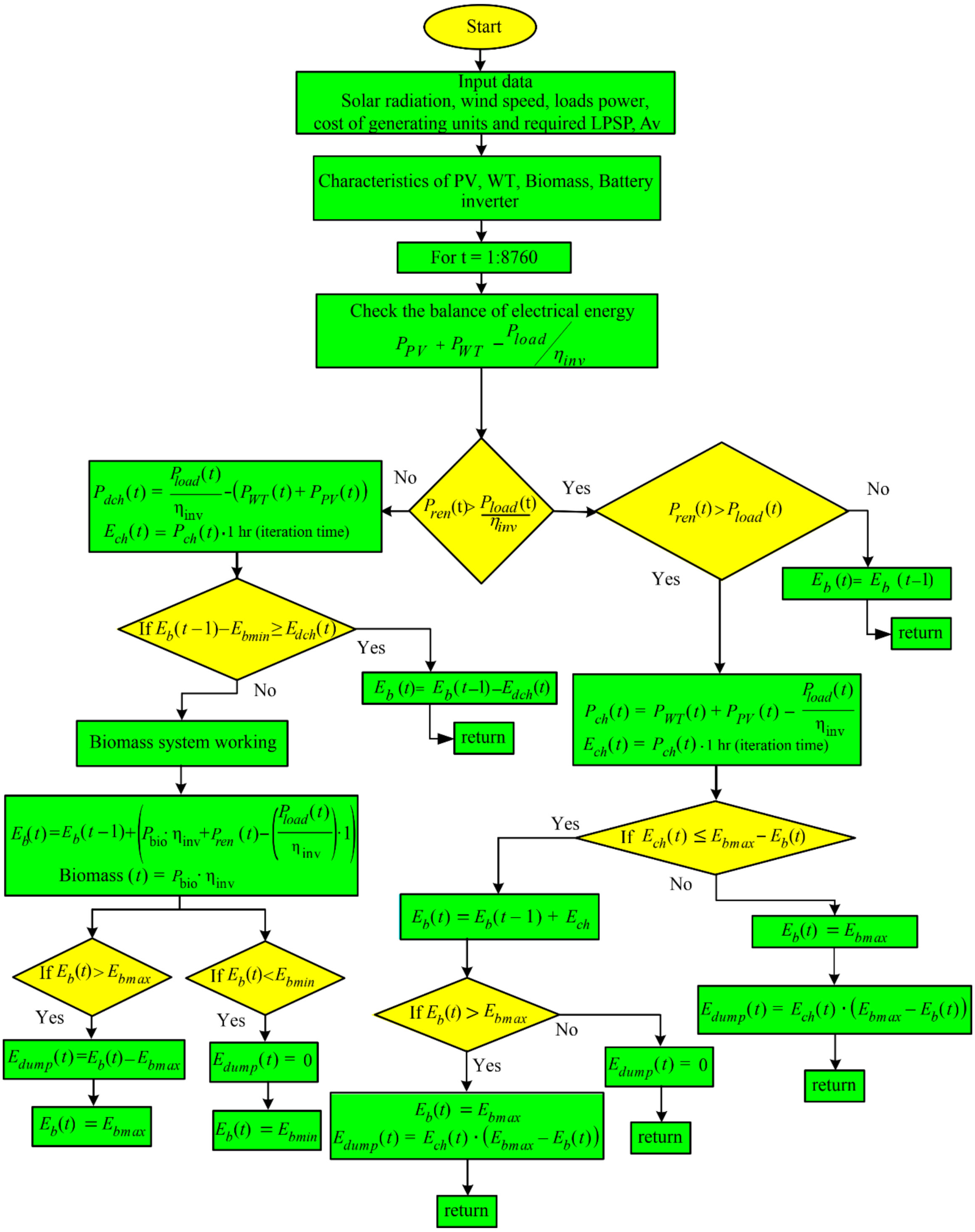

Figure 3. Power management of the *PV*/WIND/DIESEL/*BESS*.

2.2. *Wind System*

The output power of any *WT* depends mainly on the wind speed as [36]:

$$P_{wind} = \begin{cases} 0, & v\langle t\rangle \leq v_{ci},\ v\langle t\rangle \geq v_{co} \\ a \times V\langle t\rangle 3 - b \times P_r, & v_{ci} < v\langle t\rangle < v_r \\ P_r, & v_r \leq v\langle t\rangle < v_{co} \end{cases} \quad (3)$$

where, V represents the wind velocity, P_r is the rated power, V_{ci}, V_{co} and V_r are the cut-in, cut-out and rated wind speeds, respectively, a, b are two constants expressed as:

$$\begin{cases} a = P_r / \left({v_r}^3 - {v_{ci}}^3 \right) \\ b = {v_{ci}}^3 / \left({v_r}^3 - {v_{ci}}^3 \right) \end{cases} \tag{4}$$

The wind rated power is expressed as:

$$P_r = \frac{1}{2} \times \rho \times A_{wind} \times C_p \times {v_r}^3 \tag{5}$$

where, ρ represents the air density, A_{wind} is the swept area of the wind turbine, and C_p is the maximum power coefficient ranging from 0.25 to 0.45.

2.3. Biomass System

Biomass is a renewable energy system that produces power given by the expression [37]:

$$P_{BM} = \frac{T_{BM} \times 1000 \times C_{V\_BM} \times \eta_{BM}}{8760 \times O_t} \tag{6}$$

where, T_{BM} is the total organic material of biomass (Ton/year), C_{V_BM} is the calorific value of the organic material, which equals 20 MJ/kg, η_{BM} is the biomass efficiency of 24% and $\boldsymbol{O_t}$ presents the operating hours each day.

2.4. Diesel System

The diesel generator is used as a back-up source of energy, and it only works when needed. The output power of the diesel generator is calculated as [38]:

$$P_{dg} = \frac{F_{dg}\langle t \rangle - A_g \times P_{dg,out}}{B_g} \tag{7}$$

where, F_{dg} is the fuel consumption, $P_{dg,out}$ is the output power of diesel generator, A_g and B_g are constants of the linear consumption of the fuel.

2.5. BESS System

The *BESS* is a mandatory element for the isolated hybrid systems. The battery is charged when there is extra power and it is discharged when the load needs power more than the available from other sources. The capacity of *BESS* is expressed as follows [38]:

$$C_{BESS} = \frac{E_l \times AD}{DOD \times \eta_i \times \eta_b} \tag{8}$$

where, E_l is the load demand, AD represents the autonomy daily of the battery, DOD is the depth of discharge of the battery, η_{inv} and η_b are the battery and inverter efficiency, respectively.

3. Formulation of the Optimization Problem

3.1. Net Present Cost

The *NPC* is the primary factor to be considered for any project design. It is counted as a sum of all components costs, including the capital, operation & maintenance, and replacement costs, taking into account the interest rate ($\boldsymbol{i_r}$), inflation rate (δ), and escalation rate (μ). *NPC* modeling is expressed as follows [39]:

$$NPC = C + OM + R + FC_{dg} \tag{9}$$

3.1.1. *PV* and *WT* Costs

The cost modeling of *PV* and *WT* are similar. The capital cost of *PV* or *WT* ($C_{PV,WT}$) is expressed based on the initial cost ($\lambda_{PV,WT}$) and area ($A_{PV,WT}$) as follows [40]:

$$C_{PV,WT} = \lambda_{PV,WT} \times A_{PV,WT} \tag{10}$$

The operation & maintenance costs ($OM_{PV,WT}$) are expressed as:

$$OM_{PV,WT} = \theta_{PV,WT} \times A_{PV,WT} \times \sum_{i=1}^{N} \left(\frac{1+\mu}{1+i_r} \right)^{i} \tag{11}$$

where, $\theta_{PV,WT}$ is the annual operation & maintenance cost for any component, $\boldsymbol{N}$ is the project lifetime. The replacement costs are considered null because the project lifetime and the *PV* or *WT* lifetime are the same.

3.1.2. Diesel Costs

The costs of the diesel generator are modeled as follows [39]:

$$C_{dg} = \lambda_{dg} \times P_{dg} \tag{12}$$

$$OM_{dg} = \theta_{dg} \times N_{run} \times \sum_{i=1}^{N} \left(\frac{1+\mu}{1+i_r} \right)^{i} \tag{13}$$

$$R_{diesel} = R_{dg} \times P_{dg} \times \sum_{i=7,14\ldots} \left(\frac{1+\delta}{1+i_r} \right)^{i} \tag{14}$$

$$C_f(t) = p_f \times F_{dg}\langle t \rangle \tag{15}$$

$$FC_{dg} = \sum_{t=1}^{8760} C_f t \times \sum_{i=1}^{N} \left(\frac{1+\delta}{1+i_r} \right)^{i} \tag{16}$$

where, C_{dg} is the diesel investement cost, λ_{dg} is the initial diesel cost, OM_{dg} represents the operation and replacement cost, θ_{dg} is the annual *O&M* cost of diesel, N_{run} is the number of diesel-run in the year, R_{diesel} is the diesel replacement cost, R_{dg} represents the annual replacement cost of diesel, p_f is the cost of the fuel, F_{dg} is the consumed quantity of fuel and FC_{dg} is the total fuel cost.

3.1.3. *BESS* Costs

The initial and *O&M* (contain the replacement) costs of the *BESS* are expressed as follows [40]:

$$C_{BESS} = \lambda_{bat} \times C_{bat} \tag{17}$$

$$OM_{BESS} = \theta_{bat} \times C_{bat} \times \sum_{i=1}^{T_B} \left(\frac{1+\mu}{1+\delta} \right)^{(i\_1)N_{bat}} \tag{18}$$

where, λ_{bat} is the *BESS* initial cost and θ_{bat} is the annual *O&M* cost of *BESS*.

3.1.4. Biomass Costs

The biomass cost is represented as [35]:

$$C_{bg} = \lambda_{bg} \times P_{bg} \tag{19}$$

$$OM_{bg} = \theta_1 \times P_{bg} \times \sum_{i=1}^{N} \left(\frac{1+\mu}{1+i_r} \right)^{i} + \theta_2 \times P_w \times \sum_{i=1}^{N} \left(\frac{1+\mu}{1+i_r} \right)^{i} \tag{20}$$

where, λ_{bg} is the initial biomass cost, θ_1 is the annual fixed cost of *O&M*, θ_2 is the variable cost of *O&M* of biomass and P_w is the annual working of the system (kWh/Year).

3.1.5. Inverter Costs

The inverter investment and $O\&M$ costs are represented as [39]:

$$C_{inv} = \lambda_{inv} \times P_{inv} \tag{21}$$

$$OM_{Inv} = \theta_{Inv} \times \sum_{i=1}^{N} \left(\frac{1+\mu}{1+i_r} \right)^i \tag{22}$$

where, λ_{inv} is the inverter initial cost and θ_{Inv} is the annual $O\&M$ cost of the inverter.

3.2. Levelized Cost of Energy

Levelized cost of energy ($LCOE$) is a critical factor, in fact, the consumers don't care about the project cost or its lifetime, but their interest is how much they would pay for each kilowatt-hour of energy. Therefore, the $LCOE$ is a measure of the average NPC over its lifetime, and it is expressed as follows [38]:

$$LCOE = \frac{NPC \times CRF}{\sum_{t=1}^{8760} P_{load}\langle t \rangle}. \tag{23}$$

where, CRF is the capital recovery factor used to convert the initial cost to an annual capital cost, and it is expressed as:

$$CRF(ir, R) = \frac{i_r \times (1+i_r)^R}{(1+i_r)^R - 1} \tag{24}$$

3.3. Loss of Power Supply Probability

The loss of power supply probability ($LPSP$) is a technical factor used to express the reliability of the system. The $LPSP$ is expressed as follows [38]:

$$LPSP = \frac{\sum_{t=1}^{8760} \left(P_{load}\langle t \rangle - P_{pv}\langle t \rangle - P_{wind}\langle t \rangle + P_{dg,out}\langle t \rangle + E_{bmin} \right)}{\sum_{t=1}^{8760} P_{load}\langle t \rangle} \tag{25}$$

3.4. Renewable Energy Fraction

The transfer from the classical electricity production to the renewable energy project is not easy. The majority of previous work introduced renewable energies partially, while the objective here is to use 100% renewable energy. Therefore, the renewable energy factor is used to determine the percent of the renewable energy used. The renewable energy fraction (RF) is expressed as follows [38]:

$$RF = \left(1 - \frac{\sum_{t=1}^{8760} P_{dg,out}\langle t \rangle}{\sum_{t=1}^{8760} P_{re}\langle t \rangle} \right) \times 100 \tag{26}$$

where, P_{re} represents the total renewable energy power.

3.5. Availability Index Fraction

The availability index (A) predicts customer satisfaction, and it measures the energy converted to the load while confirming the ability of the project's designed system. It index is calculated as [40]:

$$A = 1 - \frac{DMN}{\sum_{t=1}^{8760} P_{load}\langle t \rangle} \tag{27}$$

$$DMN = P_{bmin}\langle t \rangle - P_b\langle t \rangle - \left(P_{pv}\langle t \rangle + P_{wind}\langle t \rangle + P_{dg,out}\langle t \rangle - P_{load}\langle t \rangle \right) \times u\langle t \rangle \tag{28}$$

where, P_{bmin} is the battery min state, P_b is the battery power at instance t, u is 1 when the load is not satisfied and 0 otherwise.

3.6. Constraints

In the suggested microgrid system, the operating constraints are:

$$\begin{array}{c} 0 \leq A_{pv} \leq A_{pv}^{max}, \\ 0 \leq A_{wind} \leq A_{wind}^{max}, \\ 0 \leq P_{dgn} \leq P_{dgn}^{max} \\ 0 \leq P_{Cap\_bat} \leq P_{Cap\_bat}^{max} \\ LPSP \leq LPSP^{max} \\ RF^{min} \leq RF, \\ A^{min} \leq A \\ \mathrm{AD}^{\mathrm{min}} \leq \mathrm{AD} \end{array} \tag{29}$$

4. Algorithms

4.1. Invasive Weed Optimization Algorithm

The IWO is a metaheuristic algorithm that has been proposed in [41]. In IWO, the social, reproductive, and competitive behaviors of the invasive weed have been modeled based on four strategies; adapting to any environment, enduring occupation of the fields, high reproduction of seeds, raise the invasive population and exclusion of the lower plant's fitness. These strategies are subjected to the conditions of the invasive weeds and the field occupied. The mathematical modeling of IWO algorithm is presented in the following subsections.

4.1.1. Population Initialization

An invasive weed is a parasite that can be created anywhere, but it is not native to this location. In the IWO algorithm, to mimic the invasive weed, a population of weeds that stochastically spread in a search space with a random position is considered.

4.1.2. Reproduction

The reproduction of weeds is an asexual form where a seed is formed without fertilization, after that, the somatic cells in the mother plant develop into an embryo. The number of seeds produced depends on the weed density. At low densities, there may not be enough pollen to produce more seeds. After the reproduction step, the search space becomes more genetically diverse, which can involve more competition.

Each member of the weed's population can produce seeds depending on its limits and capability. The population grows linearly with each iteration until they subject to a competitive selection if they exceed the maximum allowed plants in the colony. The number of seeds that a weed can produce S_i is expressed as follows:

$$S_i = S_{min} + \frac{S_{max} - S_{min}}{f_{max} - f_{min}} \times (f_i - f_{min}) \tag{30}$$

where, S_{max}, S_{min} denote the maximum and minimum number of seeds, respectively, f_{max} and f_{min} present maximum and minimum fitness values of the plants in the colony, respectively, f_i is the fitness of the plant i.

4.1.3. Spatial Dispersal

The spread of the seeds in the search space is randomly and distributed near the parent plant. However, the standard deviation σ of the random function will be reduced from a previously defined initial value, $\sigma_{\mathrm{initial}}$, to a final value, σ_{final}, in every generation, the decrease of standard deviation will allow controlling the search space. The nonlinear alteration of the standard deviation σ_{iter} is given as follows:

$$\sigma_{iter} = \frac{(iter_{max} - iter)^n}{(iter_{max})^n} \times \left(\sigma_{\mathrm{initial}} - \sigma_{final}\right) + \sigma_{final} \tag{31}$$

where, $iter_{max}$ is the maximum number of iterations, iter is the current iteration, and n is the nonlinear modulation index.

4.1.4. Competitive Exclusion

As explained before, the seeds result from asexual reproduction, and the plant invasive is very strong, which doesn't give up easily. As a result, reproduction increases, and the search space becomes more overcrowded. In the IWO, the search space has a maximum allowed of plants. When reproduction becomes unsupported, a competitive exclusion operation is implemented. The competition between plants is introduced in the IWO algorithm to exclude the exceeds of the maximum allowed number from the plants included weeds and seeds in a colony. The exclusion is applied through a mechanism that eliminates the plants with low fitness in the colony based on a ranked list contains both weeds and seeds. The idea is to let just the strong weeds because they have the most chance of survival and reproduction contrariwise of the poor fitness plants.

The overall steps of IWO algorithm are shown in Algorithm 1.

Algorithm 1: IWO

```
Initialize a set of random weeds, weed_B^i = (weed_B^1, weed_B^2, ..., weed_B^N) within the limits
weed_min^i ≤ weed_B^i ≤ weed_max^i.
Set the IWO's parameters
Evaluate the objective function for all weeds
   While (iter < iter_max)
            Calculate the best and worst fitness in the colony
             Calculate the σ
             for each weed in the colony
             Calculate the number of seeds following the
             fitness of each weed
             Add the seeds to their parents in the colony
                    if Size_max ≤ Nb_population
             Sort the new population according to their fitness
             Eliminate the worst fitness in order to achieve the Size_max allowed
                    end if
               end for
   Update iteration  iter = iter + 1
end while
Return the final best solution
```

4.2. Backtracking Search Algorithm

BSA is a new optimization algorithm that has been proposed for solving real-valued numerical optimization problems [42]. In BSA, unlike the other evolutionary algorithms, it's mitigating several problems as excessive sensitivity to control parameters, premature convergence, and slow computation. As a result, BSA has only one parameter. Moreover, BSA's performance is not overly sensitive to the initial value of this parameter. BSA's population is generated based on the genetic operators presented in the selection, mutation, and crossover. Moreover, the search-direction matrix and search-space boundaries' amplitude control gives it potent exploration and exploitation capabilities. BSA has a particularity to use a memory containing a random population, which can share its experience for the next generation to guide the search-direction in the best way.

4.2.1. Population Initialization

The population is a sum of individuals which are spread uniformly in the search space. It can be expressed as:

$$P_{i,j} \sim \mathrm{U}\Big(\mathrm{low}_j,\ \mathrm{up}_j\Big) \tag{32}$$

where, *i* and *j* denote the population size and problem dimension, respectively, low and up denote the lower and upper values of each individual, U expresses the uniform distribution in each individual.

4.2.2. Selection-I

BSA's Selection-I step is dedicated to the memory data used to get a better direction. The memory is called the historical population *oldP*. The initial historical population is determined randomly as:

$$oldP_{i,j} \sim \mathrm{U}\left(\mathrm{low}_j,\ \mathrm{up}_j\right) \tag{33}$$

In BSA, the *oldP* is redefining at the beginning of each iteration through the 'if-then' expressed in (34):

$$if\ a < b\ then\ oldP\ :=\ P|a, b\ \sim (0\ ,\ 1) \tag{34}$$

where := is the update operation, Equation (34) ensures that BSA designates a population belonging (historical population) and remembers those until it changed. After that, the order of individuals in *oldP* is randomly changed using a shuffling function as in Equation (35):

$$oldP\ := permuting(oldP) \tag{35}$$

4.2.3. Mutation

The mutation is a genetic operator used to maintain the genetic diversity of chromosomes, and it is analogous to biological mutation. The mutation alters one or more gene values in the chromosome. BSA's mutation process is expressed as follows:

$$Mutant = P + F.(oldP - P) \tag{36}$$

where, F controls the amplitude of the search-direction matrix, *oldP-P*.

4.2.4. Crossover

The crossover, also called recombination, is a genetic operator used to combine two parents' genetic information to generate new offspring T. In BSA's, the crossover is the last step to generate the trial offspring, it has two steps. The first step calculates the binary integer-valued matrix (map) that indicates the individuals of T to be manipulated using the relevant individuals of P, for the second one when the map equals to 1, then T update the p-value. The overall steps of BSA algorithm are shown in Algorithm 2.

4.3. Hybrid IWO/BSA Algorithm

As with any population-based algorithm, IWO has some problems concerning the competitive capability where the seeds are not taken care of their capacities. As a result, IWO has not good results in the convergence compared with the other algorithms. This proposed IWO/BSA algorithm aims to help the seeds take good fitness, which involves the competitivity in the colony of weeds. The proposed strategy is adapted to subject the seeds to the backtracking search method operators based on the genetic operators denoted in the selection, mutation, and crossover. The BSA algorithm allows involving the global exploration while IWO is giving the best exploitation.

He proposed IWO-BSA algorithm is based on the following steps, initialization, reproduction, then, the generated seeds are treated using the BSA operators as, Selection I (to select the current and historical populations), mutation, crossover, Selection II (to select the optimal population), spatial dispersal and competitive exclusion.

4.3.1. Initialization

The IWO/BSA algorithm population is a set of invasive plants (weeds); the population is randomly spread in the search space.

4.3.2. Reproduction

As like in the IWO algorithm, the reproduction of weeds is an operation based on an asexual generation of seeds without fertilization. The seeds number generated of each weed is calculated using Equation (30).

Algorithm 2: BSA

Initialize a set of random population $P_i = (X_1, X_2, \ldots, X_N)$ and historical population $oldP_i = (X_1, X_2, \ldots, X_N)$ within the limits $X^i_{min} \le X \le X^i_{max}$.
Initialize set the only BSA parameter called the mix rate and take the best fitness at the inf value.
Evaluate the objective function for the P_i.
While ($iter < iter_{max}$)
    Selection-I look at equations 24,25 and 26
Mutation calculates mutant using: $Mutant = P + F.(oldP - P)$ where F = 0.6 randn
    Crossover calculates the trial population T:
    $map^j_i = zeros$
        if (c < d | c, d $\sim U(0\ ,\ 1)$) then
            for i from 1 to N do
        $map(i, u(1 : mixrate.rand.dim)) = 0 \mid u = \ permuting((1, 2 \ldots D))$
            end
        else
        for i from 1 to N do, $map(i, randi(D)) = 0$
        end
    Generate the Trial population, T $:= mutant$
        for i from 1 to N do
            for i from 1 to N do
                if $map_{i,j} = 1$ then $T_{i,j} \ := P_{i,j}$
            end
        end
    Appling the Boundary Control Mechanism
    Selection-II evaluate the objective function of T_i
        for i from 1 to N do
if $fitness\ T_i < fitness\ P_i$ then
                $fitness\ P_i = fitness\ T_i$
                $P_i = \ T_i$
            end
        end
    Comparison between the actual best solution P_{best} and P_i
end while
Return the final best solution P_{best}

4.3.3. Selection I

The selection-I in IWO/BSA is dedicated to select the historical population and the current population, as presented in Equation (33). To strengthen the plants, they are modeled as chromosomes. The somatic cells of the seed each contain 24 chromosomes (12 maternal and 12 paternal).

4.3.4. Mutation and Crossover

Mutation and crossover is a genetic operator used to maintain the genetic diversity of chromosomes and it is analogous to biological mutation. The mutation alters one or more gene values in the chromosome. It is implemented like in BSA.

4.3.5. Spatial Dispersal

The dispersion of the new seeds is coming after submitting them to the BSA operators. The dispersion is randomly in the search space and distributed as an IWO algorithm. However, the standard deviation σ of the random function is also calculated using Equation (31).

4.3.6. Competitive Exclusion

After the dispersion in the search space, this later becomes more overcrowded. It has a maximum allowed of weeds, which should implement a strategy called competitive exclusion to decrease the colony's number of elements. However, in this stage, a competitivity between weeds appears. The weeds are classed based on their own fitness, and then, the low fitness will be excluded. This strategy is used in IWO algorithm which used a mechanism to eliminate the low weeds fitness.

4.3.7. Selection II

In the Selection-II stage, a weed with a better fitness value than the others is selected as the best global solution. Also, in this stage, we upload the best local solution. The summarized process is shown in Figure 4, while Figure 5 shows the proposed IWO/BSA algorithm's main flowchart.

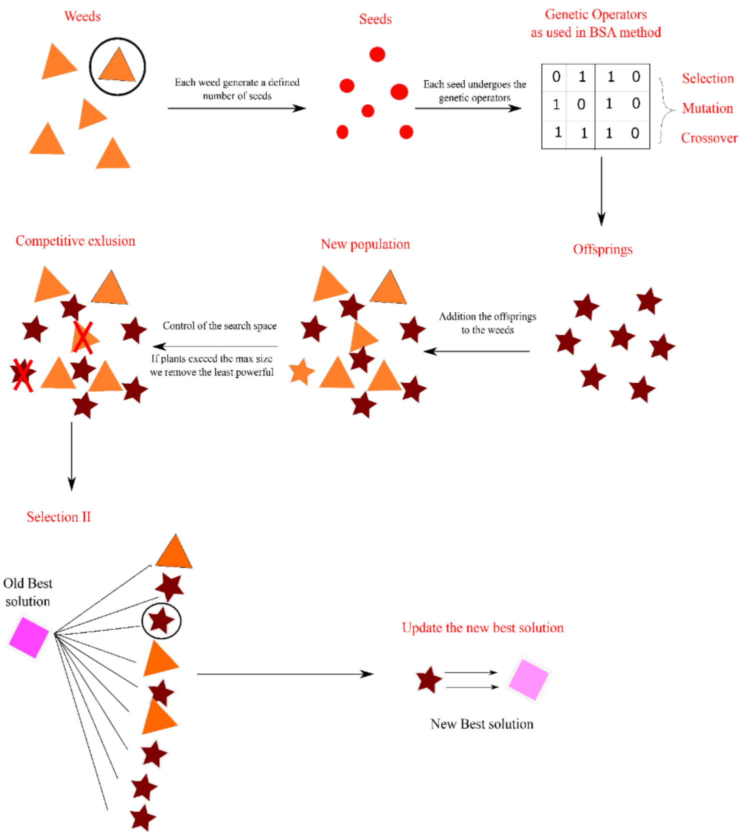

Figure 4. Proposed IWO/BSA algorithm process.

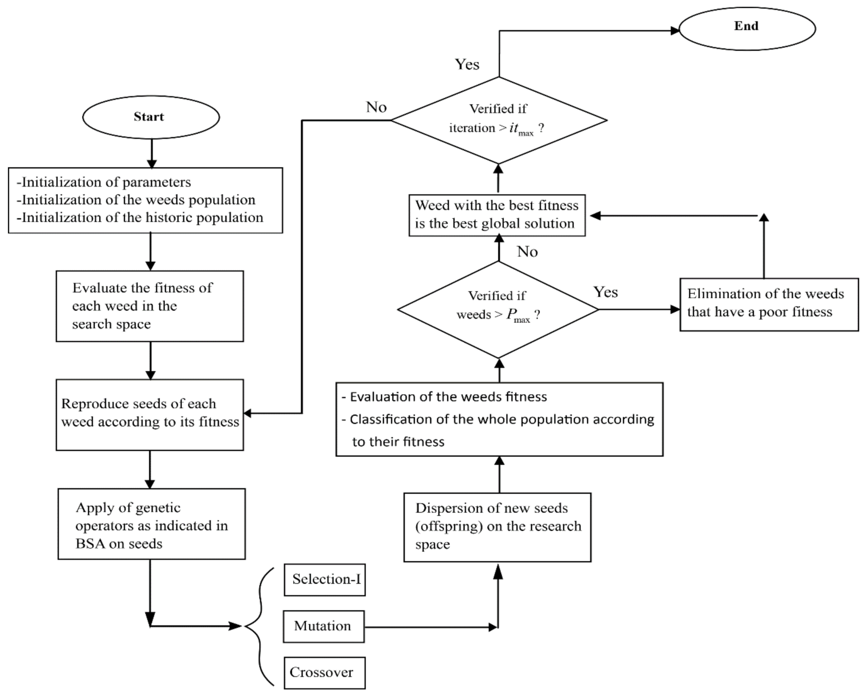

Figure 5. Flowchart of the proposed IWO/BSA algorithm.

5. Case Study

To validate the robustness of the proposed IWO/BSA algorithm, it is utilized for determining the optimal sizing of the proposed hybrid renewable system, which consists of different configurations. These proposed configurations are the *PV*/wind turbine/biomass/battery, *PV*/biomass, *PV*/diesel generator/battery, and wind turbine/diesel generator/battery systems. The proposed hybrid systems have been introduced in the isolated mode to satisfy the proposed site's load requirements. The project is applied in Dakhla (Morocco), as shown in Figure 6. The annual load curve for one hour is shown in Figure 7. Figure 8a–d present the solar irradiation, temperature, wind speed, and pressure, respectively. Four standalone system scenarios will be evaluated for covering the load demand in that site, wherein each kind, four different configurations of the hybrid system are studied. These configurations are: (1) *PV*/wind/biomass/battery, (2) *PV*/biomass, (3) *PV*/diesel/battery and (4) wind/diesel/battery systems. The proposed IWO/BSA is validated on optimal sizing of these four hybrid systems, and the optimization results are comprehensively compared with the corresponding ones obtained from AEFA, GWO, BSA, and IWO algorithms. The dumped power is used in an electrical heater with the aim of heating the water for house use.

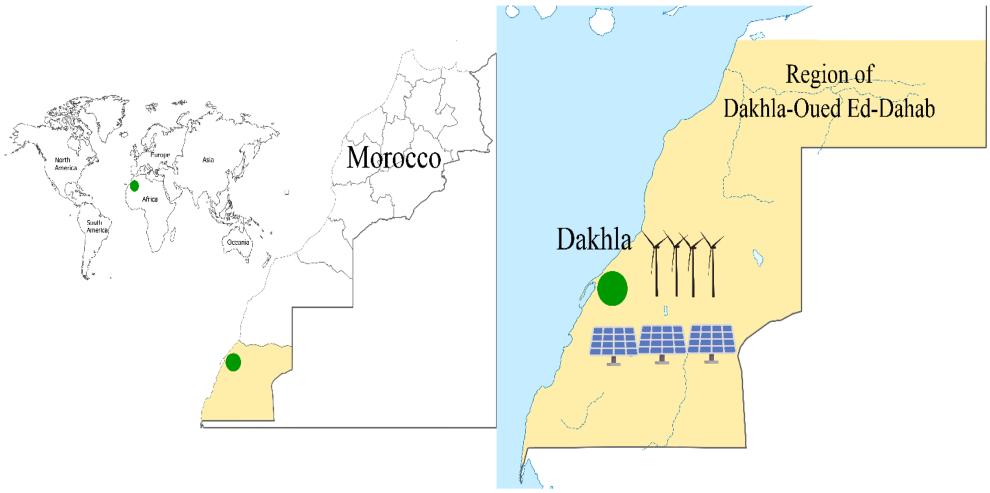

Figure 6. Dakhla map.

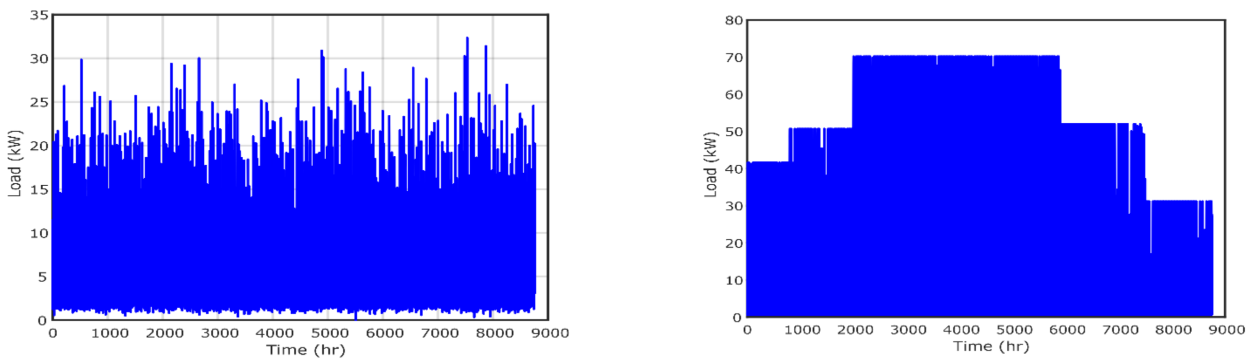

(**a**) Load for the *PV*/wind/biomass/battery system

(**b**) Load for the *PV*/biomass system

Figure 7. *Cont.*

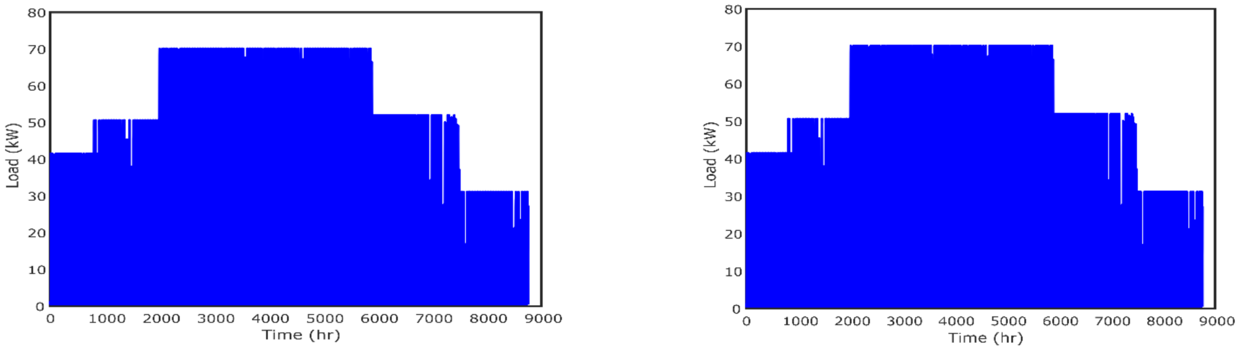

(**c**) Load for the *PV*/diesel/battery system (**d**) Load for the Wind/diesel/battery system

Figure 7. Hourly load power in the four houses.

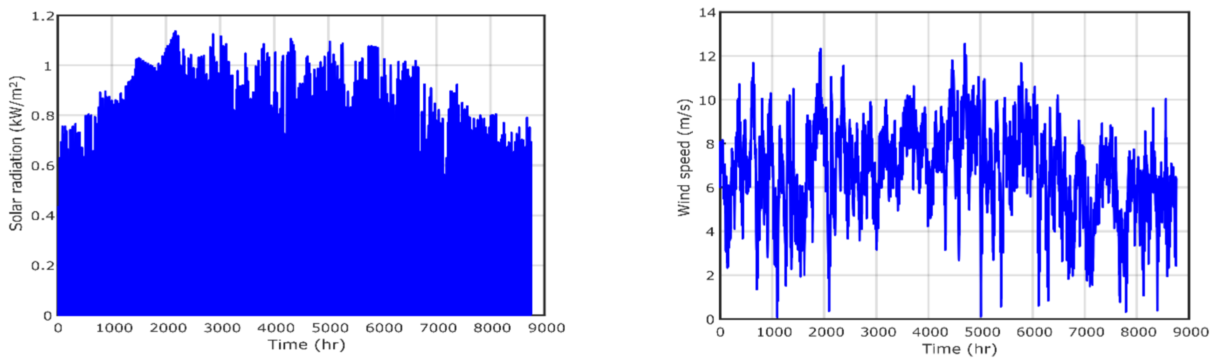

(**a**) Solar irradiation. (**c**) Wind speed.

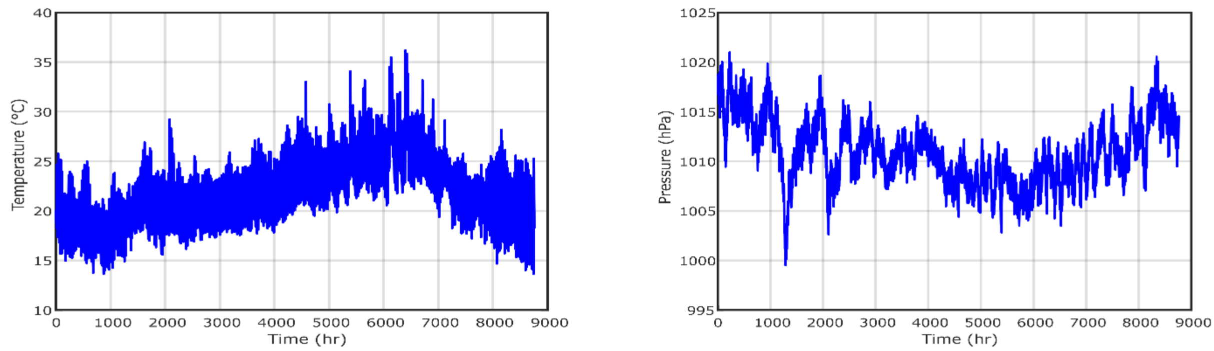

(**b**) Temperature. (**d**) Pressure.

Figure 8. Meteorological conditions.

6. Results and Discussion

In this section, the optimal design of a proposed hybrid renewable system is achieved using the developed IWO/BSA algorithm. The effectiveness of the proposed algorithm on the suggested system is validated via different scenarios and cases. The optimal sizing is based on minimizing the *NPC* as an objective function, while the parameters of optimization are: (i) the *PV* area, (ii) the swept area of the wind turbine, (iii) the rated power of diesel generator, (iv) the nominal capacity of the battery, and (V) the biomass capacity. To confirm the suitability of the proposed IWO/BSA in addressing the studied optimization problem, IWO/BSA, AEFA, GWO, BSA, and IWO are launched 100 times for each configuration and a statistical study is conducted based on a set of measures like the best minimum value of the fitness function. For an in-depth analysis of the obtained results and to ensure the analysis study, four indices are calculated, the *NPC*, *LCOE*, *LPSP*, and the availability. In the next subsections, the optimization results are provided for the standalone system with multiple scenarios. Modeling and simulation of the optimization problem have been accomplished using MATLAB 2015a program, while the adjusted parameters are the same for all studied configurations and the input data are presented in Table A1 in the Appendix A, likewise the algorithms parameters are presented in Table A2, i.e., the number of maximum iterations is taken as 100 iterations and the search agents' number is 10. The results of the statistical measurements for the proposed IWO/BSA and the other algorithms, AEFA, GWO, BSA and IWO are listed in Tables 2 and 3. From these tables, the reader can conclude that the IWO/BSA technique generates the best minimum value of the fitness function in all cases. The convergence curves of the 100 iterations for all the studied configurations using IWO/BSA, AEFA, GWO, BSA, and IWO are shown in Figure 9. From this figure, it can be observed that the convergence characteristics of developed IWO/BSA are better than those obtained by the other optimization algorithms.

Table 2. Optimal sizing obtained by the proposed algorithm for the studied scenarios.

Hybrid Power System	Algorithm	*PV* (m^2)	*WT* (m^2)	Diesel (kW)	Battery (kWh)	Biomass (t/Year)
PV/*WT*/Biomass/Battery	AEFA	67.5137	702.9344	//	4.7888	32.1741
	GWO	77.4342	780.7906	//	9.2082	27.5612
	BSA	75.7053	576.7633	//	4.8753	0.3522
	IWO	234.6187	890.4494	//	6.8913	19.6979
	IWO/BSA	89.7678	554.205	//	4.78773	0.0000
PV/Biomass	AEFA	355.5057	//	//	//	32.3361
	GWO	357.6068	//	//	//	34.2460
	BSA	390.6575	//	//	//	0.6572
	IWO	386.4402	//	//	//	50.2505
	IWO/BSA	349.5524	//	//	//	18.9940
PV/Diesel/Battery	AEFA	414.1790	//	0.6979	13.1553	//
	GWO	436.8411	//	0.5732	21.4832	//
	BSA	385.4886	//	0.5367	11.5347	//
	IWO	488.2624	//	0.5697	27.8874	//
	IWO/BSA	391.3988	//	0.5565	12.9746	//
WT/Diesel/Battery	AEFA	//	7440.8018	0.0949	11.9624	//
	GWO	//	8481.7017	0.9766	23.9765	//
	BSA	//	2237.7688	48.2904	11.9192	//
	IWO	//	2124.2369	54.1864	29.9514	//
	IWO/BSA	//	1850.8162	20.8737	41.5201	//

Table 3. Indices obtained by the proposed algorithm of all scenarios.

Hybrid Power System	Algorithm	*NPC* ($)	*LCOE* ($/kWh)	*LPSP*	Availability (%)	Renewable Energy (%)	Battery Autonomy (Day)
PV/*WT*/Biomass/Battery	AEFA	132,529	0.3048	0.0487	96.7275	//	0.5025
	GWO	147,645	0.3395	0.0494	96.9305	//	0.9663
	BSA	112,324	0.2583	0.0496	95.8039	//	0.5116
	IWO	201,912	0.4643	0.0372	97.3849	//	0.7232
	IWO/BSA	111,929	0.2574	0.0498	95.7752	//	0.5024
PV/Biomass	AEFA	127,339	0.1210	0.0484	96.0199	//	//
	GWO	128,009	0.1216	0.0477	96.1075	//	//
	BSA	130,611	0.1241	0.0500	95.1179	//	//
	IWO	136,344	0.1295	0.0393	96.9598	//	//
	IWO/BSA	124,689	0.1184	0.0499	95.6296	//	//

Table 3. *Cont.*

Hybrid Power System	Algorithm	*NPC* ($)	*LCOE* ($/kWh)	*LPSP*	Availability (%)	Renewable Energy (%)	Battery Autonomy (Day)
PV/Diesel/Battery	AEFA	164,695	0.1565	0.0433	97.1636	98.6270	0.5703
	GWO	166540	0.1582	0.0456	97.3848	98.9496	0.9313
	BSA	151,667	0.1441	0.0498	96.6089	98.8330	0.5000
	IWO	168,305	0.1599	0.0278	98.7587	99.1402	1.2089
	IWO/BSA	142,233	0.1354	0.0250	98.6109	98.8330	0.5635
WT/Diesel/Battery	AEFA	839,754	0.7977	0.0491	95.6578	99.9995	0.5186
	GWO	967,611	0.9192	0.0497	96.0061	99.9959	1.0394
	BSA	1,084,283	1.0300	0.0494	99.6037	98.6116	0.5167
	IWO	1,178,630	1.1197	0.0234	99.8091	98.2891	1.2984
	IWO/BSA	590,097	0.5606	0.0128	96.5619	99.1954	1.7999

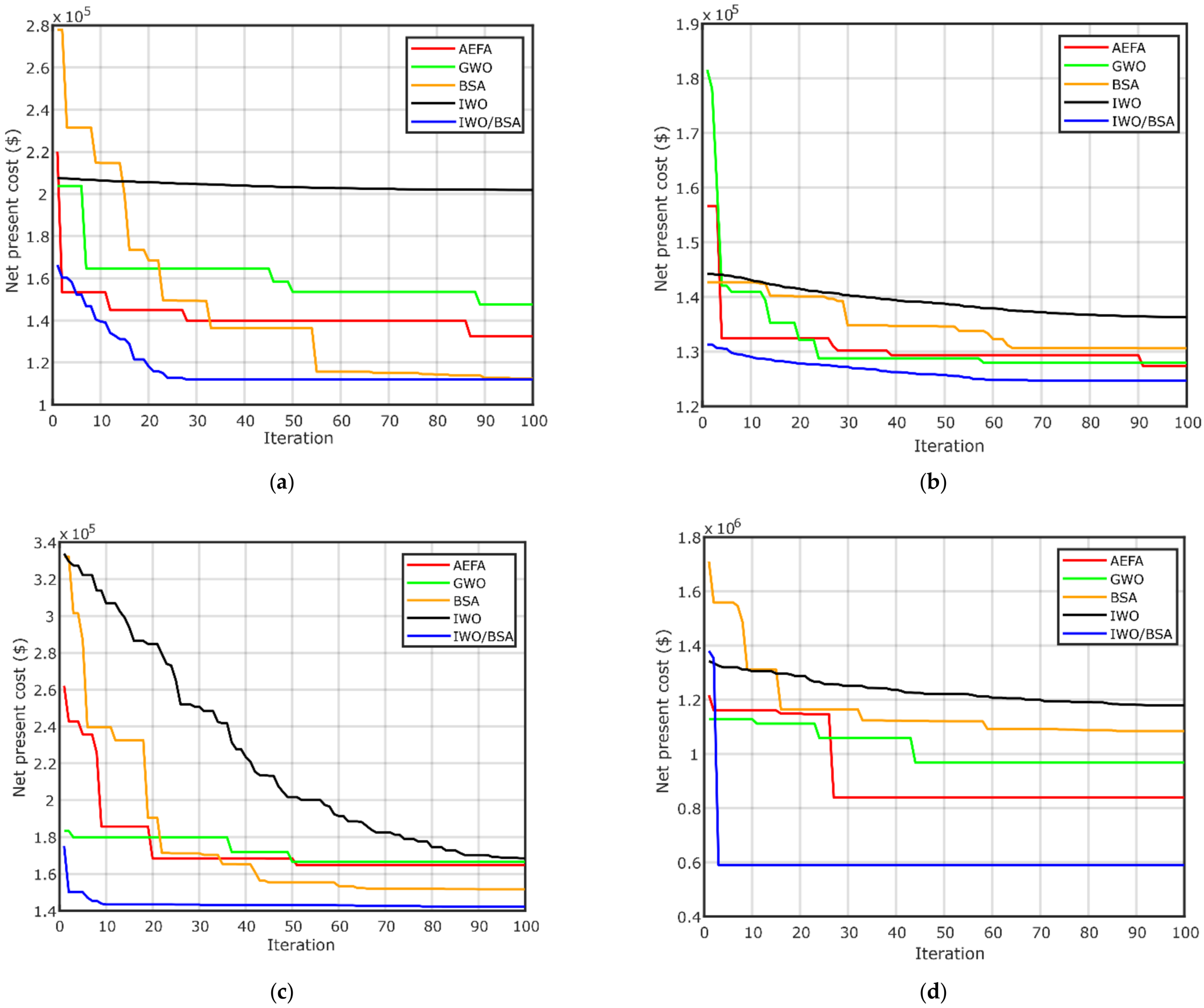

Figure 9. The *NPC* convergence using the proposed AEFA, GWO, BSA, IWO and the proposed IWO/BSA for all scenarios, (**a**) *PV*/*WT*/biomass/battery, (**b**) *PV*/biomass, (**c**) *PV*/diesel/battery, (**d**) *WT*/diesel/battery.

The results of the statistical measurements for the proposed IWO/BSA, compared with the AEFA, GWO, IWO and BSA algorithms, are listed in Tables 2 and 3. From Table 2, the reader can conclude that the proposed IWO/BSA algorithm gives the best results for all scenarios. It can also be observed that the hybrid *PV*/*WT*/Biomass/Battery system shows a high competitivity using IWO/BSA algorithm. The *NPC* of the obtained optimized system is 111929 USD, with an *LCOE* of 0.2574 USD; likewise, the constraints are satisfied, and the project is 100% with renewable sources.

Tables 2 and 3 present the results obtained by the developed algorithm, the net present cost function, the optimized parameters results, i.e., (A_{pv}, A_{wind}, P_{dgn}, P_{Cap_bat}, P_{BM}) for all suggested configurations. From Figure 9, the reader can notice that using IWO/BSA, AEFA, GWO, BSA and IWO algorithms, the best minimum values of the objective function (*NPC*) is obtained for the first configuration, i.e., hybrid *PV*/*WT*/Biomass/Battery. From Table 3, it can be observed that IWO/BSA gives the minimum value of *NPC* in all cases. The datasheet of technologies is presented in Table A3 in the Appendix A.

Figure 10 shows the output power of the studied systems through annual power management. Figure 10a, shows the output power of the *PV*/*WT*/Biomass/Battery, where the power from the wind turbine represents the important contribution which reaches 90% as shown in Figure 11a. Otherwise, the *PV* represents only 9% of power contribution, and the biomass is not considered in the optimized system. Figure 10b shows the output power of the *PV*/biomass system, where it can be observed that the biomass is considered a back-up and presents only 1% of total power production percent Figure 11b. Figure 10c, shows the annual output power of the *PV*/diesel/battery system, it is observed that the main unit is the *PV* system with 97% as shown in the Figure 11c, while the diesel generator contributes to 1% power production. Figure 10d, shows the annual generated power of the *WT*/diesel/battery system, where the wind system generates 98% of the power, while the battery and diesel systems used as a back-up, and they don't pass more than 1% of the power generation as shown in Figure 11d.

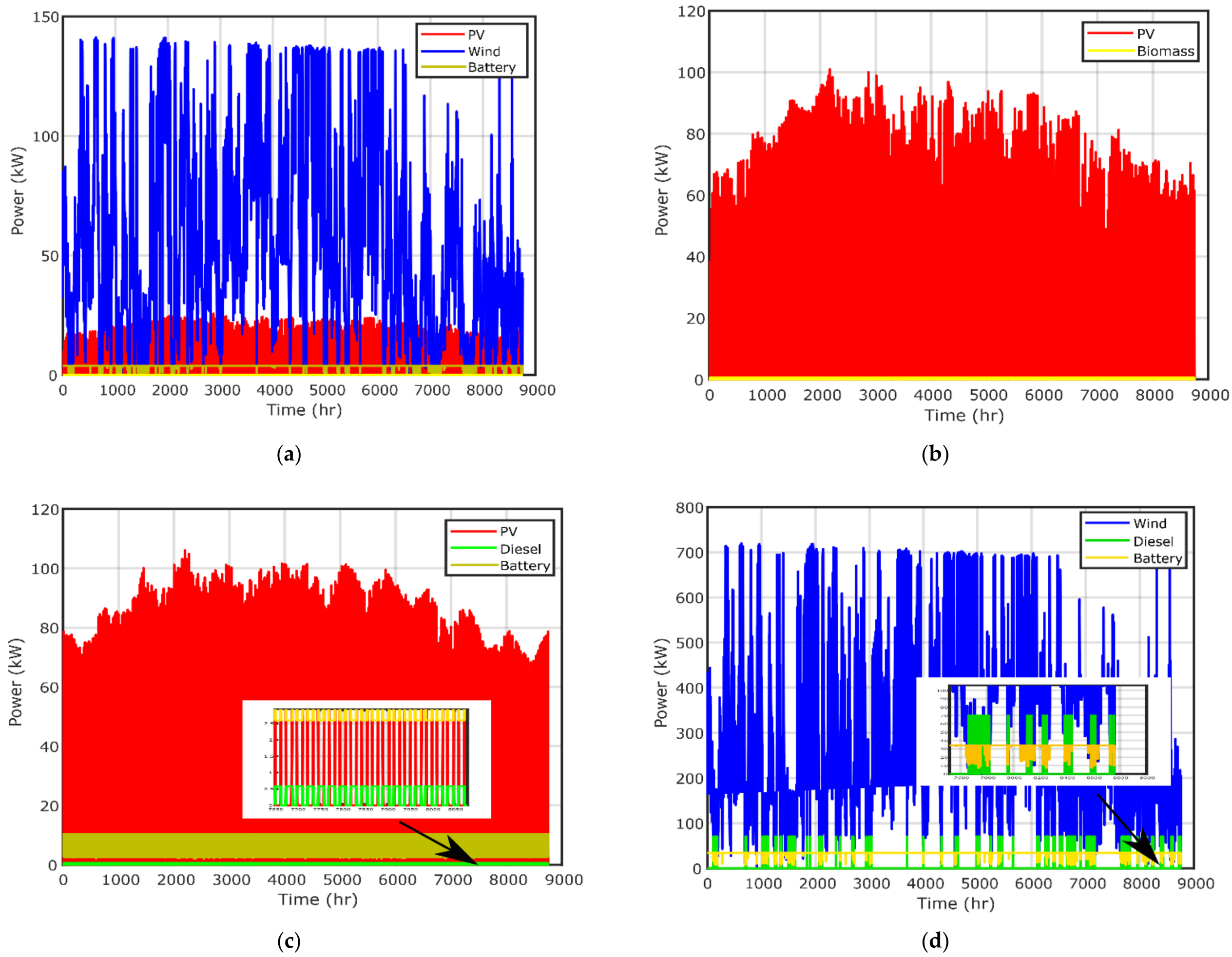

Figure 10. Annual contribution of *PV*, wind, battery, diesel, and biomass obtained by the proposed IWO/BSA algorithm, for scenarios (**a**) *PV*/*WT*/biomass/battery, (**b**) *PV*/biomass, (**c**) *PV*/diesel/battery, (**d**) *WT*/diesel/battery.

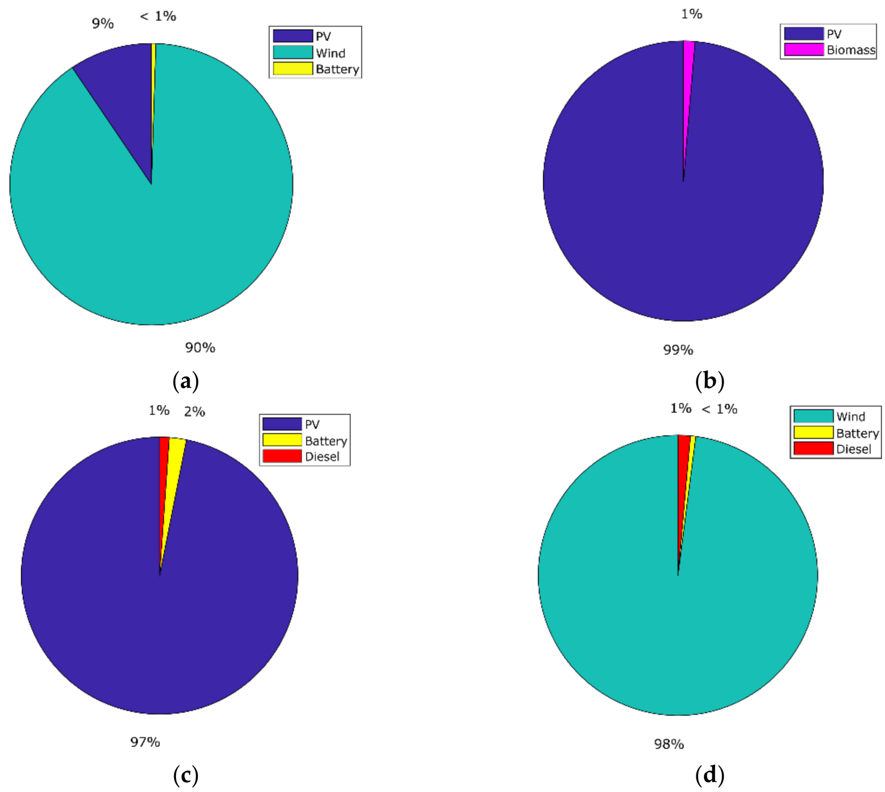

Figure 11. Annual contribution of *PV*, *WT*, battery, and diesel and biomass obtained by the proposed IWO/BSA algorithm, (**a**) *PV*/*WT*/biomass/battery, (**b**) *PV*/biomass, (**c**) *PV*/diesel/battery, (**d**) *WT*/diesel/battery.

Figure 12 shows the time-response of *PV*, *WT*, battery, diesel generator, biomass, load powers obtained via the proposed IWO/BSA algorithm for all scenarios during some hours. The figures show the hourly generated power between 2200 to 2500. Figure 12a, shows the time response of the *PV*, wind, biomass, battery, and load powers. It is observed that the power from the wind is dumped, while the power from the *PV* feeds the load. Figure 12b, shows the time response of the *PV*, biomass, and load powers, where the dumped power is null. Figure 12c, shows the time response of the *PV*, diesel, battery and load powers. It is observed that the *PV* is the pillar of the system, while the diesel is considered as a back-up. Figure 12d, shows the time response of the wind, battery, diesel, and load powers, where it is observed a significant dumped power generated by the wind turbine.

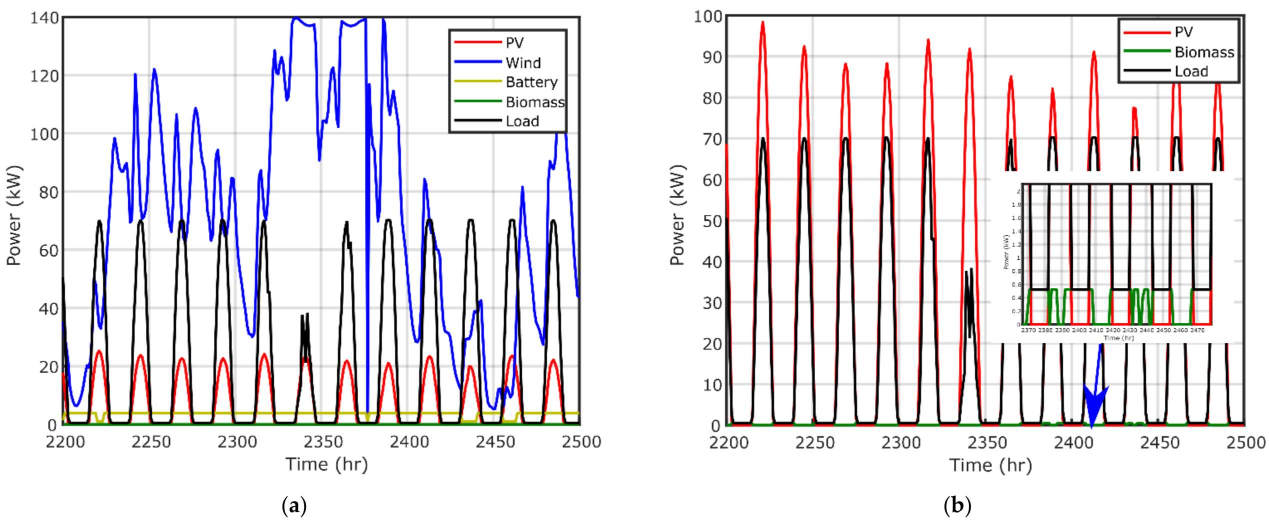

Figure 12. *Cont.*

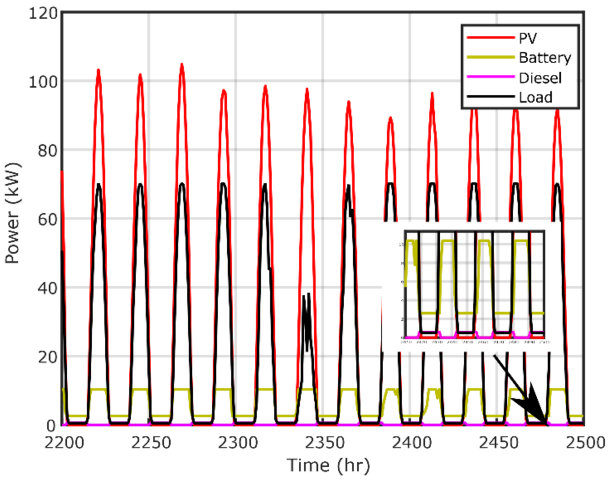

(**c**)

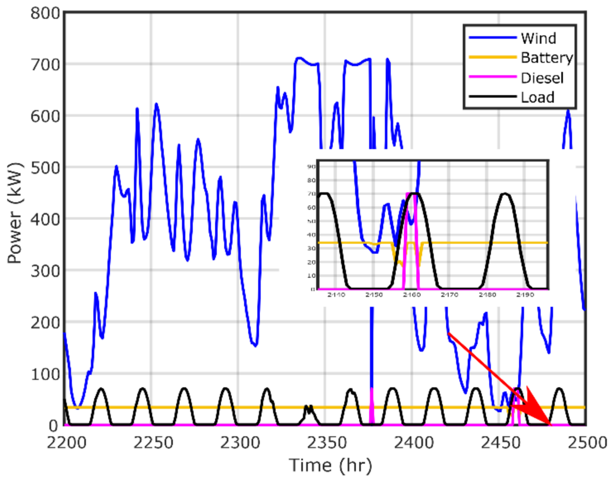

(**d**)

Figure 12. Time-response of *PV*, *WT*, battery, diesel generator, biomass, load powers obtained via the proposed IWO/BSA algorithm for all scenarios during some hours, (**a**) *PV*/*WT*/Biomass/Battery, (**b**) *PV*/Biomass, (**c**) *PV*/Diesel/Battery, (**d**) *WT*/Diesel/Battery.

Figure 13 shows the state of charge (SOC) in the three cases when the battery is used. In Figure 13a,c, the SOC is mostly charged because the systems have the wind turbine system. In Figure 13b, the SOC is a square signal, because the battery is charged in the sunniest time and discharge in the inverse. This frequency in each day presents a square signal form. Otherwise, Figure 14 shows the battery's charge and discharge for the studied configurations.

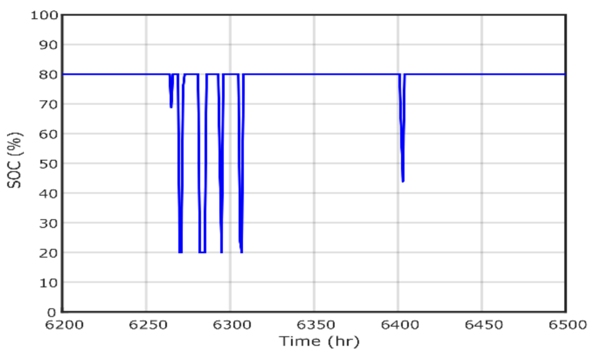

(**a**)

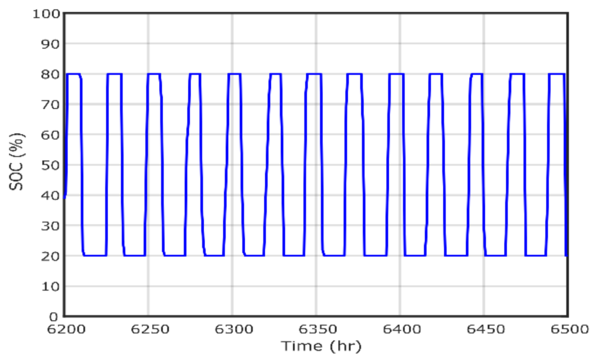

(**b**)

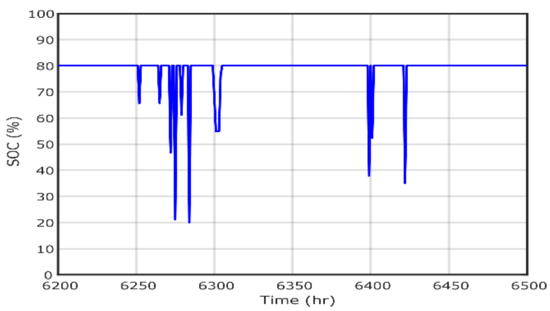

(**c**)

Figure 13. State of charge of battery in scenarios, (**a**) *PV*/*WT*/biomass/battery, (**b**) *PV*/diesel/battery, (**c**) *WT*/diesel/battery.

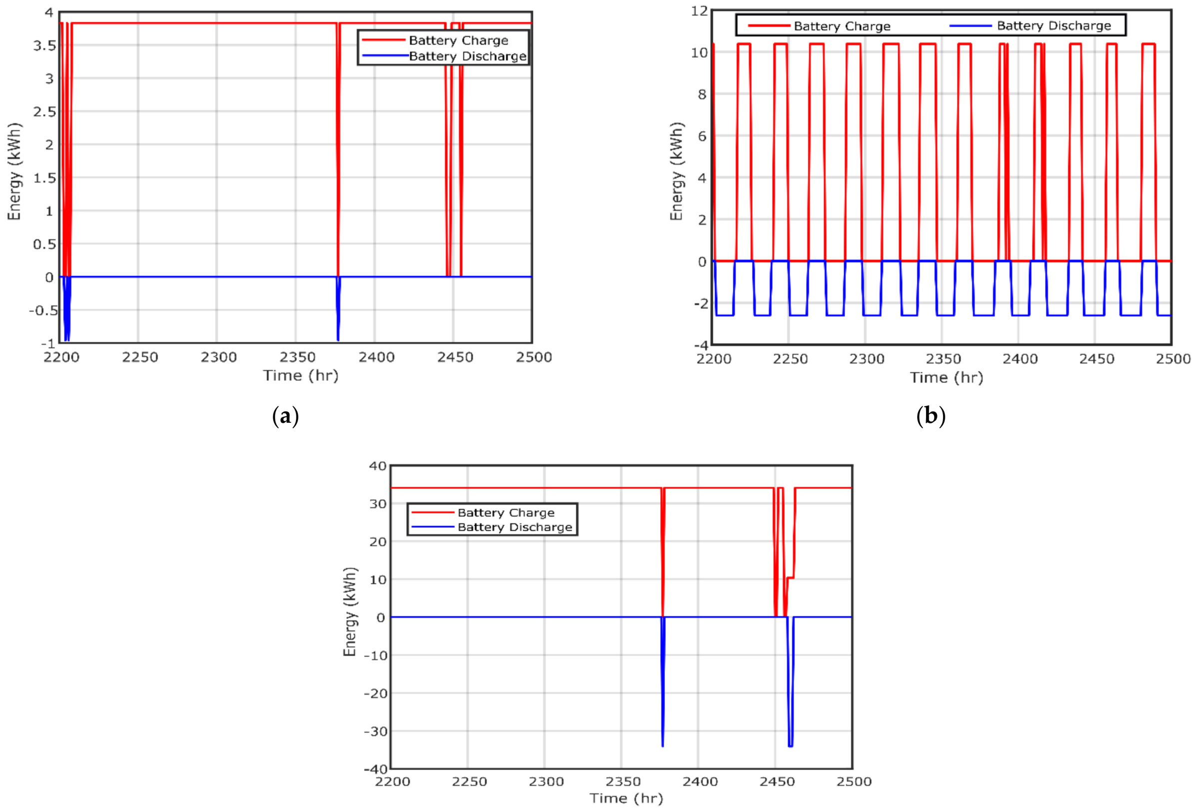

(**a**) (**b**) (**c**)

Figure 14. Charge and discharge of battery in scenarios, (**a**) *PV*/*WT*/biomass/battery, (**b**) *PV*/diesel/battery, (**c**) *WT*/diesel/battery.

The proposed IWO/BSA algorithm is extensively examined with different case studies and scenarios. The IWO/BSA algorithm gives the best results compared with alternatives for all studied scenarios. The main results can be summarized as follows; the best HMGs in the Dakhla region is the *PV*/biomass with an *LCOE* of 0.1184 $. The best algorithm in all case studies is the proposed IWO/BSA algorithm compared with AEFA, GWO, IWO, and BSA.

7. Conclusions

This paper has proposed a hybrid optimization algorithm, called IWO/BSA, with the aim of improving the performance of the original IWO and BSA algorithms by combining their advantages into an algorithm. The proposed algorithm has been applied for the optimal economic design of a stand-alone hybrid microgrid system in Dakhla (Morocco). Four configurations consist of RES (*PV*, *WT* and biomass) with diesel generators and battery storage systems have been suggested. The obtained results showed that the *PV*/Biomass scenario is the most cost-effective system with an *LCOE* of 0.1184 $/kWh; otherwise, the best configuration of the microgrid system contained 349.55 m^2 of *PV* and 18.9940 ton/year consumed by the biomass system; the *PV*/diesel/*BESS* scenario is also cost-effective with *LCOE* of 0.1354 $/kWh. On the other side, the *LPSP* and availability index are satisfied without the need for traditional resources. Additionally, the results showed the proposed IWO/BSA algorithm's ability to reach the optimal solution compared with the original IWO and BSA, and other recent algorithms in all studied cases. The obtained results from this study would be useful material for decision-makers working on developing the renewable energy sector in the Moroccan Sahara region in south Morocco. In the current paper, the parameter tuning of studied optimization algorithms has not been taken into account. In the future work, the parameter tuning of each algorithm could be carried out using Taguchi technique. In addition, it is suggested to apply the proposed IWO/BSA for solving other complex optimization problems.

Author Contributions: Conceptualization, M.K., S.K. and R.E.; Data curation, M.A.-A., A.S.A. and M.A.; Formal analysis, A.E., and M.I.M.; Resources, A.E., M.I.M.; Methodology, M.A.-A., A.S.A. and M.A.; Software, M.K., S.K. and R.E.; Supervision, A.E., and M.I.M.; Validation, M.K. and S.K.; Visualization, M.A.-A., A.S.A. and M.A.; Writing—original draft, M.K., S.K., R.E., M.A.-A., and A.S.A.; Writing—review & editing, M.A., A.E. and M.I.M. All authors together organized and refined the manuscript in the present form. All authors have read and agreed to the published version of the manuscript.

Funding: This research was funded by the deputyship for Research & Innovation Ministry of Education in Saudi Arabia grant number IFP-2020-06.

Institutional Review Board Statement: Not applicable.

Informed Consent Statement: Not applicable.

Acknowledgments: The authors extend their appreciation to the deputyship for Research & Innovation Ministry of Education in Saudi Arabia for funding this research work through the project number (IFP-2020-06).

Conflicts of Interest: The authors declare no conflict of interest.

Abbreviations

AEFA	Artificial Electric Field Algorithm
ALO	Antlion Optimizer
BESS	Battery energy storage system
BO	Bonobo Optimizer
BOACA	Bi-objective ant colony algorithm
BSA	Backtracking Search Algorithm
COE	Cost of Energy
CS	Cuckoo search
CSA	Crow search algorithm
DG	Diesel generator
FA	Firefly algorithm
GA	Genetic algorithm
GC	Grid-Connected
GOA	Grasshopper Optimization Algorithm
GWO	Grey Wolf Optimizer
HHO	Harris Hawks optimizer
HRES	Hybrid renewable energy system
IWO	Invasive Weed Optimization
JLBO	Jaya and teaching–learning-based optimization
MPPT	Maximum Power Point Tracker
MVO	Multi-Verse Optimizer
NPC	Net Present Cost
PHS	Pumped hydro storage
PSO	Particle swarm optimization
QOBO	Quasi-Oppositional Bonobo Optimizer
RES	Renewable energy sources
SA	Stand-Alone
SOC	State of charge
SSO	Social spider optimizer
TORSCHE	Time Optimization of Resources, Scheduling
WDO	Wind driven optimization
WOA	Whale Optimization Algorithm
WT	Wind turbine

Symbols

$A_{PV,WT}$	Area of PV and swept area of wind (m^2)
A_g, B_g	Constants of the linear consumption of the fuel (L/kW)
A_{pv}	PV area (m^2)
A_{wind}	Swept area of the wind turbine (m^2)
C_{BESS}	Capacity of $BESS$ (kWh)
C_{BESS}	Initial cost of the $BESS$ ($)
$C_{PV,WT}$	Investment cost of PV and wind generators ($)
C_{V_BM}	Calorific value of the organic material (MJ/kg)
C_{bat}	Capacity of battery (kWh)
C_{bg}	Investment cost of biomass ($)
$C_f(t)$	Cost of the consumed quantity of fuel ($/year)
C_{inv}	Inverter investment cost ($)
C_p	Maximum power coefficient (%)
E_{bmin}	Min battery energy in discharge (kWh)
E_l	Energy Load (kWh)
FC_{dg}	Fuel cost ($)
F_{dg}	Fuel consumption (L/h)
$F_{dg}(t)$	Consumed quantity of fuel (L)
N_{run}	Diesel run number
OM_{BESS}	$O\&M$ (contain the replacement) costs of the $BESS$ ($)
OM_{Inv}	$O\&M$ cost of the inverter ($)
$OM_{PV,WT}$	Operation & maintenance costs ($)
OM_{bg}	$O\&M$ cost of biomass ($)
OM_{dg}	Maintenance and Operation cost of diesel generator ($)
O_t	Operating hours (hr)
P_{BM}	Biomass power (kW)
P_{bg}	Rated capacity of biomass (kW)
$P_{dg,out}$	Output power of diesel generator (kW)
$P_{dg,out}$	Output power of diesel generator (kW)
P_{dg}	Output power of diesel generator (kW)
P_{inv}	Rated power of the inverter (kW)
P_{load}	Load power (kW)
P_{pv}	Output power of PV (kW)
P_r	Rated power (kW)
P_{re}	Output power of renewable energy sources (kW)
P_w	Annual working of system (kWh/Year)
P_{wind}	Output wind power (kW)
R_{dg}	Annual replacement cost of diesel ($)
R_{diesel}	Diesel replacement cost ($/kW)
S_i	Number of seeds that a weed can produce
S_{max}	Maximum allowed number of seeds generated
S_{min}	Minimum allowed number of seeds generated
T_{BM}	Total organic material of biomass (t/yr)
T_a	Ambient temperature (°C),
T_r	Photovoltaic cell reference temperature (°C).
f_i	Fitness of the plant i
f_{max}	Maximum fitness value of the plants in the colony
f_{min}	Minimum fitness value of the plants in the colony
i_r	Interest rate (%)
$iter_{max}$	Maximum iteration
p_f	Fuel price ($/L)
v_{ci}	Cut-in speed (m/s)
v_{co}	Cut-out speed (m/s)
v_r	Rated wind speed (m/s)
η_{BM}	Biomass efficiency (%)
η_b	Efficiency of the battery (%)
η_i	Efficiency of the inverter (%)

η_{pv}	Efficiency of the *PV* (%)
η_r	Reference efficiency, η_t is the efficiency of the MPPT equipment,
θ_1	Annual fixed cost of *O&M* of biomass ($/kW/year)
θ_2	Variable cost of *O&M* of biomass ($/kWh)
θ_{Inv}	Annual *O&M* cost of the inverter ($/year)
$\theta_{PV,WT}$	Annual operation & maintenance of *PV* and wind ($/m^2/year)
θ_{bat}	Annual *O&M* cost of *BESS* ($/m^2/year)
θ_{dg}	Annual *O&M* cost of diesel ($/hr)
$\lambda_{PV,WT}$	Initial cost of *PV* and wind ($/m^2)
λ_{bat}	*BESS* initial cost ($/kWh)
λ_{bg}	Biomass initial cost ($/kW)
λ_{dg}	Diesel initial cost ($/kW)
λ_{inv}	Inverter initial cost ($/m^2)
σ_{initial}	Initial standard deviation
σ_{final}	Final standard deviation
σ_{iter}	Standard deviation
A	Availability index (%)
AD	Autonomy daily of the battery (day)
C	Investment cost ($)
CRF	Capital recovery factor
DOD	Depth of discharge (%)
I	Solar irradiation (kW/m^2)
$LCOE$	Levelized cost of energy ($/kWh)
$LPSP$	Loss of power supply probability (%)
$NOCT$	Nominal operating cell temperature (°C),
NPC	Net Present Cost ($)
OM	Operation and maintenance cost ($)
R	Replacement cost ($)
RF	Renewable Fraction (%)
n	Nonlinear modulation index
v	Wind velocity (m/s)
β	Temperature coefficient of the efficiency
δ	Inflation rate (%)
μ	Escalation rate (%)
ρ	Air density (Kg/m^3)

Appendix A

Table A1. Summary of the HRES parameters.

Symbol	Quantity	Conversion
N	Project lifetime	20 year
i_r	Interest rate	13.25%
μ	Escalation rate	2%
δ	Inflation rate	12.27%
λ_{pv}	*PV* initial cost	300 $/m^2
θ_{pv}	Annual *O&M* cost of *PV*	$0.01 * \lambda_{pv}$ $/m^2/year
η_r	Reference efficiency of the *PV*	25%
η_t	Efficiency of MPPT	100%
T_r	*PV* cell reference temperature	25 °C
β	Temperature coefficient	0.005 °C
$NOCT$	Nominal operating cell temperature	47 °C
N_{pv}	*PV* system lifetime	20 year
λ_{wind}	Wind initial cost	125 $/m^2
θ_{wind}	Annual *O&M* cost of wind	$0.01 * \lambda_{wind}$ $/m^2/year
C_{p_wind}	Maximum power coefficient	48%
V_{ci}	Cut-in wind speed	2.6 m/s
V_{co}	Cut-out wind speed	25 m/s
V_r	Rated wind speed	9.5 m/s

Table A1. *Cont.*

Symbol	Quantity	Conversion
N_{wind}	Wind system lifetime	20 year
λ_{dg}	Diesel initial cost	250 $/kW
θ_{dg}	Annual *O&M* cost of diesel	0.05 $/h
R_{dg}	Replacement cost	210 $/kW
p_f	Fuel price in Egypt	0.43 $/L
N_{diesel}	Diesel system lifetime	7 year
λ_{bat}	Battery initial cost	100 $/kWh
θ_{bat}	Annual operation & maintenance cost of Battery	$0.03 * \lambda_{bat}$ $/m^2/year
DOD	Depth of discharge	80%
η_b	Battery efficiency	97%
SOC_{min}	Minimum state of charge	20%
SOC_{max}	Maximum state of charge	80%
N_{bat}	Battery system lifetime	5 year
λ_{inv}	Inverter initial cost	400 $/m^2
θ_{inv}	Annual *O&M* cost of inverter	20 $/year
η_{inv}	Inverter efficiency	97%

Table A2. Used parameters of Algorithms.

Algorithms	Parameters
AEFA	$K_0 = 500$; $\alpha = 30$; Population size = 10; Maximum iteration = 100
GWO	a = Linear reduction from 2 to 0; Search agents = 10; Maximum iteration = 100
IWO	$Seed_{min} = 1$; $Seed_{max} = 3$; $\sigma_{initial} = 0.5$; $\sigma_{final} = 0.001$; Population Size = 10; Maximum Population Size = 25; Exponent = 1; Maximum iteration = 100
BSA	DIM_RATE = 1; Population size = 10; Maximum iteration = 100
IWO/BSA	$Seed_{min} = 1$; $Seed_{max} = 3$; $\sigma_{initial} = 0.5$; $\sigma_{final} = 0.001$; Exponent = 1; DIM_RATE = 1; Population Size = 10; Maximum Population Size = 25; Maximum iteration = 100

Table A3. Datasheet of technologies.

System	Datasheet
PV	Manufacture: Solar World; Model: Submodule Plus SW 255 poly; Rated power: 255 W; Area: 1.68 m^2
Wind Biomass	Manufacture: Siemens; Model: S*WT*-3.0-113; Rated power: 3 kW; Area: 10,029 m^2 Community Power Corporation (CPC)
Diesel	Rated power: 140 W
Battery	Model: Lead Acid, Rated power: 1.85 kWh
Inverter	Manufacture: Sunny Swiss, Model: SB2000HF, Nominal power: 8000 W

References

1. Babatunde, O.M.; Munda, J.L.; Hamam, Y. A Comprehensive State-of-the-Art Survey on Hybrid Renewable Energy System Operations and Planning. *IEEE Access* **2020**, *8*, 75313–75346. [CrossRef]
2. Kharrich, M.; Mohammed, O.H.; Mohammed, Y.S.; Akherraz, M. A Review on Recent Sizing Methodologies for Hybrid Microgrid Systems. *Int. J. Energy Convers.* **2019**, *7*, 230–240. [CrossRef]
3. Zia, M.F.; Benbouzid, M.; Elbouchikhi, E.; Muyeen, S.M.; Techato, K.; Guerrero, J.M. Microgrid Transactive Energy: Review, Architectures, Distributed Ledger Technologies, and Market Analysis. *IEEE Access* **2020**, *8*, 19410–19432. [CrossRef]
4. Mbungu, N.T.; Naidoo, R.M.; Bansal, R.C.; Vahidinasab, V. Overview of the Optimal Smart Energy Coordination for Microgrid Applications. *IEEE Access* **2019**, *7*, 163063–163084. [CrossRef]
5. Gomes, L.; Vale, Z.A.; Corchado, J.M. Multi-Agent Microgrid Management System for Single-Board Computers: A Case Study on Peer-to-Peer Energy Trading. *IEEE Access* **2020**, *8*, 64169–64183. [CrossRef]

6. Shrestha, A.; Bishwokarma, R.; Chapagain, A.; Banjara, S.; Aryal, S.; Mali, B.; Thapa, R.; Bista, D.; Hayes, B.P.; Papadakis, A.; et al. Peer-to-Peer Energy Trading in Micro/Mini-Grids for Local Energy Communities: A Review and Case Study of Nepal. *IEEE Access* **2019**, *7*, 131911–131928. [CrossRef]
7. Mazzeo, D.; Matera, N.; de Luca, P.; Baglivo, C.; Congedo, P.M.; Oliveti, G. A literature review and statistical analysis of photovoltaic-wind hybrid renewable system research by considering the most relevant 550 articles: An upgradable matrix literature database. *J. Clean. Prod.* **2021**, *295*, 126070. [CrossRef]
8. Diab, A.A.Z.; Sultan, H.M.; Mohamed, I.S.; Kuznetsov, O.N.; Do, T.D. Application of Different Optimization Algorithms for Optimal Sizing of *PV*/Wind/Diesel/Battery Storage Stand-Alone Hybrid Microgrid. *IEEE Access* **2019**, *7*, 119223–119245. [CrossRef]
9. Zhou, Z.; Ge, L. Operation of Stand-Alone Microgrids Considering the Load Following of Biomass Power Plants and the Power Curtailment Control Optimization of Wind Turbines. *IEEE Access* **2019**, *7*, 186115–186125. [CrossRef]
10. Kharrich, M.; Mohammed, O.; Akherraz, M. Design of Hybrid Microgrid *PV*/Wind/Diesel/Battery System: Case Study for Rabat and Baghdad. *EAI Endorsed Trans. Energy Web* **2018**, *7*, 162692. [CrossRef]
11. Tooryan, F.; HassanzadehFard, H.; Collins, E.R.; Jin, S.; Ramezani, B. Optimization and energy management of distributed energy resources for a hybrid residential microgrid. *J. Energy Storage* **2020**, *30*, 101556. [CrossRef]
12. Bukar, A.L.; Tan, C.W.; Lau, K.Y. Optimal sizing of an autonomous photovoltaic/wind/battery/diesel generator microgrid using grasshopper optimization algorithm. *Solar Energy* **2019**, *188*, 685–696. [CrossRef]
13. Sanajaoba, S. Optimal sizing of off-grid hybrid energy system based on minimum cost of energy and reliability criteria using firefly algorithm. *Solar Energy* **2019**, *188*, 655–666. [CrossRef]
14. Fathy, A.; Kaaniche, K.; Alanazi, T.M. Recent Approach Based Social Spider Optimizer for Optimal Sizing of Hybrid *PV*/Wind/Battery/Diesel Integrated Microgrid in Aljouf Region. *IEEE Access* **2020**, *8*, 57630–57645. [CrossRef]
15. Saravanan, B.; Vasudevan, E.R.; Kothari, D.P. Unit commitment problem solution using invasive weed optimization algorithm. *Int. J. Electr. Power Energy Syst.* **2014**, *55*, 21–28. [CrossRef]
16. Bhattacharjee, K.; Bhattacharya, A.; Dey, S.H.N. Backtracking search optimization based economic environmental power dispatch problems. *Int. J. Electr. Power Energy Syst.* **2015**, *73*, 830–842. [CrossRef]
17. Panda, M.R.; Das, P.; Pradhan, S. Hybridization of IWO and IPSO for mobile robots navigation in a dynamic environment. *J. King Saud Univ. Comput. Inf. Sci.* **2020**, *32*, 1020–1033. [CrossRef]
18. Mahto, S.K.; Choubey, A. A novel hybrid IWO/WDO algorithm for nulling pattern synthesis of uniformly spaced linear and non-uniform circular array antenna. *AEU Int. J. Electron. Commun.* **2016**, *70*, 750–756. [CrossRef]
19. Lin, Q.; Gao, L.; Li, X.; Zhang, C. A hybrid backtracking search algorithm for permutation flow-shop scheduling problem. *Comput. Ind. Eng.* **2015**, *85*, 437–446. [CrossRef]
20. Khan, A.; Javaid, N. Jaya Learning-Based Optimization for Optimal Sizing of Stand-Alone Photovoltaic, Wind Turbine, and Battery Systems. *Engineering* **2020**, *6*, 812–826. [CrossRef]
21. Kharrich, M.; Mohammed, O.H.; Kamel, S.; Selim, A.; Sultan, H.M.; Akherraz, M.; Jurado, F. Development and Implementation of a Novel Optimization Algorithm for Reliable and Economic Grid-Independent Hybrid Power System. *Appl. Sci.* **2020**, *10*, 6604. [CrossRef]
22. Makhdoomi, S.; Askarzadeh, A. Optimizing operation of a photovoltaic/diesel generator hybrid energy system with pumped hydro storage by a modified crow search algorithm. *J. Energy Storage* **2020**, *27*, 101040. [CrossRef]
23. Abo-Elyousr, F.K.; Elnozahy, A. Bi-objective economic feasibility of hybrid micro-grid systems with multiple fuel options for islanded areas in Egypt. *Renew. Energy* **2018**, *128*, 37–56. [CrossRef]
24. Ming, M.; Wang, R.; Zha, Y.; Zhang, T. Multi-Objective Optimization of Hybrid Renewable Energy System Using an Enhanced Multi-Objective Evolutionary Algorithm. *Energies* **2017**, *10*, 674.
25. Mohamed, A.A.; Ali, S.; Alkhalaf, S.; Senjyu, T.; Hemeida, A.M. Optimal Allocation of Hybrid Renewable Energy System by Multi-Objective Water Cycle Algorithm. *Sustainability* **2019**, *11*, 6550. [CrossRef]
26. Crainz, M.; Curto, D.; Franzitta, V.; Longo, S.; Montana, F.; Musca, R.; Riva Sanseverino, E.; Telaretti, E. Flexibility Services to Minimize the Electricity Production from Fossil Fuels. A Case Study in a Mediterranean Small Island. *Energies* **2019**, *12*, 3492. [CrossRef]
27. Hossain, M.A.; Chakrabortty, R.K.; Ryan, M.J.; Pota, H.R. Energy management of community energy storage in grid-connected microgrid under uncertain real-time prices. *Sustain. Cities Soc.* **2021**, *66*, 102658. [CrossRef]
28. Curto, D.; Franzitta, V.; Viola, A.; Cirrincione, M.; Mohammadi, A.; Kumar, A. A renewable energy mix to supply small islands. A comparative study applied to Balearic Islands and Fiji. *J. Clean. Prod.* **2019**, *241*, 118356. [CrossRef]
29. Tsai, C.-T.; Beza, T.M.; Molla, E.M.; Kuo, C.-C. Analysis and Sizing of Mini-Grid Hybrid Renewable Energy System for Islands. *IEEE Access* **2020**, *8*, 70013–70029. [CrossRef]
30. Rehman, S.; Natrajan, N.; Mohandes, M.; Alhems, L.M.; Himri, Y.; Allouhi, A. Feasibility Study of Hybrid Power Systems for Remote Dwellings in Tamil Nadu, India. *IEEE Access* **2020**, *8*, 143881–143890. [CrossRef]
31. Hossain, M.; Mekhilef, S.; Olatomiwa, L. Performance evaluation of a standalone *PV*-wind-diesel-battery hybrid system feasible for a large resort center in South China Sea, Malaysia. *Sustain. Cities Soc.* **2017**, *28*, 358–366. [CrossRef]
32. Mazzeo, D.; Baglivo, C.; Matera, N.; Congedo, P.M.; Oliveti, G. A novel energy-economic-environmental multi-criteria decision-making in the optimization of a hybrid renewable system. *Sustain. Cities Soc.* **2020**, *52*, 101780. [CrossRef]

33. Curto, D.; Favuzza, S.; Franzitta, V.; Musca, R.; Navia, M.A.N.; Zizzo, G. Evaluation of the optimal renewable electricity mix for Lampedusa island: The adoption of a technical and economical methodology. *J. Clean. Prod.* **2020**, *263*, 121404. [CrossRef]
34. Ahmad, S.; Ullah, I.; Jamil, F.; Kim, D. Toward the Optimal Operation of Hybrid Renewable Energy Resources in Microgrids. *Energies* **2020**, *13*, 5482. [CrossRef]
35. Heydari, A.; Askarzadeh, A. Optimization of a biomass-based photovoltaic power plant for an off-grid application subject to loss of power supply probability concept. *Appl. Energy* **2016**, *165*, 601–611. [CrossRef]
36. Guangqian, D.; Bekhrad, K.; Azarikhah, P.; Maleki, A. A hybrid algorithm based optimization on modeling of grid independent biodiesel-based hybrid solar/wind systems. *Renew. Energy* **2018**, *122*, 551–560. [CrossRef]
37. Sawle, Y.; Gupta, S.C.; Bohre, A.K. Socio-techno-economic design of hybrid renewable energy system using optimization techniques. *Renew. Energy* **2018**, *119*, 459–472. [CrossRef]
38. Ramli, M.A.M.; Bouchekara, H.R.E.H.; Alghamdi, A.S. Optimal sizing of *PV*/wind/diesel hybrid microgrid system using multi-objective self-adaptive differential evolution algorithm. *Renew. Energy* **2018**, *121*, 400–411. [CrossRef]
39. Movahediyan, Z.; Askarzadeh, A. Multi-objective optimization framework of a photovoltaic-diesel generator hybrid energy system considering operating reserve. *Sustain. Cities Soc.* **2018**, *41*, 1–12. [CrossRef]
40. Ghiasi, M. Detailed study, multi-objective optimization, and design of an AC-DC smart microgrid with hybrid renewable energy resources. *Energy* **2019**, *169*, 496–507. [CrossRef]
41. Mehrabian, A.R.; Lucas, C. A novel numerical optimization algorithm inspired from weed colonization. *Ecol. Inform.* **2006**, *1*, 355–366. [CrossRef]
42. Civicioglu, P. Backtracking Search Optimization Algorithm for numerical optimization problems. *Appl. Math. Comput.* **2013**, *219*, 8121–8144. [CrossRef]